

Supplementary Material for “Nonreciprocal Photon Blockade”

Ran Huang¹, Adam Miranowicz^{2,3}, Jie-Qiao Liao¹, Franco Nori^{2,4}, and Hui Jing^{1,*}

¹*Key Laboratory of Low-Dimensional Quantum Structures and Quantum Control of Ministry of Education, Department of Physics and Synergetic Innovation Center for Quantum Effects and Applications, Hunan Normal University, Changsha 410081, China*

²*Theoretical Quantum Physics Laboratory, RIKEN Cluster for Pioneering Research, Wako-shi, Saitama 351-0198, Japan*

³*Faculty of Physics, Adam Mickiewicz University, 61-614 Poznań, Poland*

⁴*Physics Department, The University of Michigan, Ann Arbor, Michigan 48109-1040, USA*

Here, we present technical details on nonreciprocal photon blockade (PB) in a driven Kerr-type model with a Fizeau drag. Our discussion includes: (1) single- (1PB) and two-photon blockade (2PB) effects; (2) our analytical solutions for the steady-state optical-intensity correlation functions; and (3) rotation-induced quantum nonreciprocity.

S1. KERR-TYPE INTERACTION WITH THE FIZEAU DRAG

To realize nonreciprocal photon blockade, we consider a rotating optical resonator with a nonlinear Kerr medium which can be described by a Kerr-type interaction with a Fizeau drag term,

$$\hat{H}_R = \hbar(\omega_0 + \Delta_F)\hat{a}^\dagger\hat{a} + \hbar U\hat{a}^\dagger\hat{a}^\dagger\hat{a}\hat{a}. \quad (\text{S1})$$

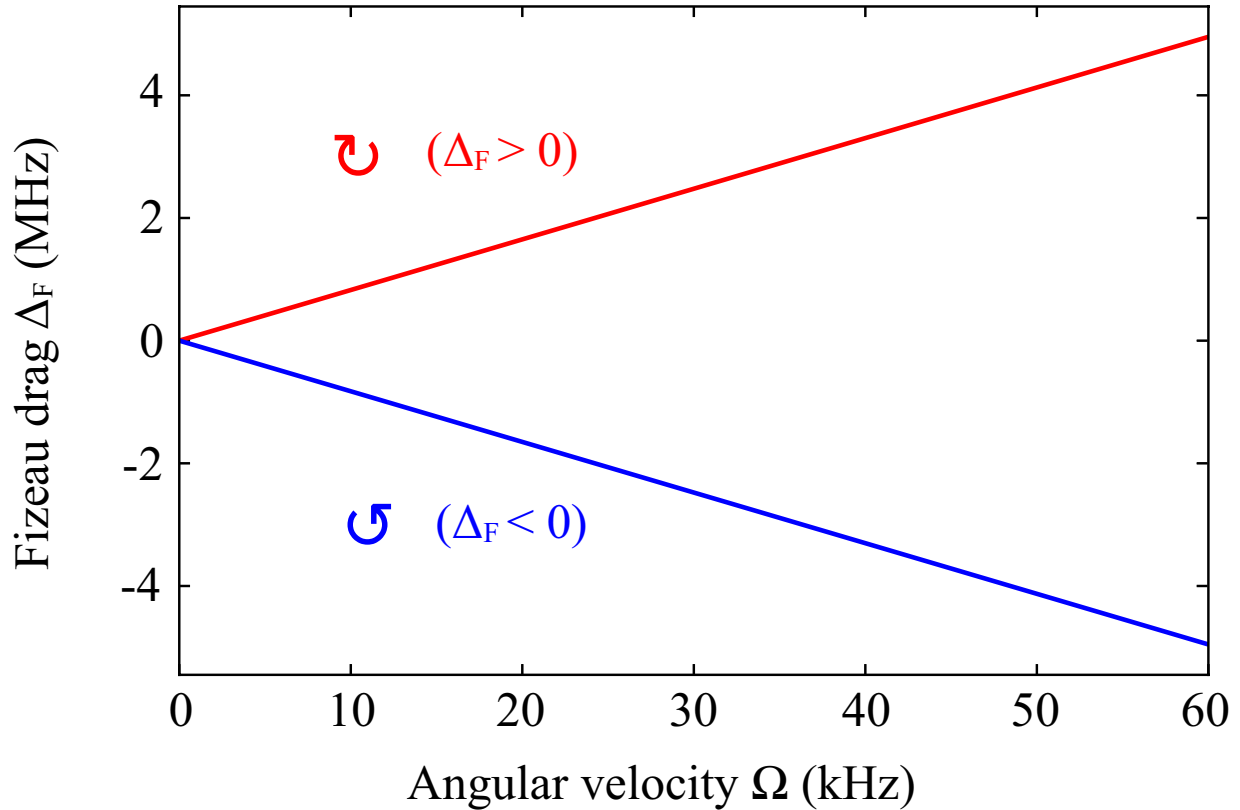


FIG. S1. Fizeau drag Δ_F versus angular velocity of the resonator for $\Delta_F > 0$ (red line) and $\Delta_F < 0$ (blue line) cases. The optical wavelength is $\lambda = 1550$ nm, the radius of the resonator is $R = 30$ μm , and the linear refractive index of the resonator is $n = 1.4$.

Here, $U\hat{a}^\dagger\hat{a}^\dagger\hat{a}\hat{a}$ is the standard Kerr interaction term [S1–S4], \hat{a} (\hat{a}^\dagger) is the annihilation (creation) operator for the cavity field, while $U = \hbar\omega_0^2cn_2/(n_0^2V_{\text{eff}})$ is the strength of the nonlinear interaction with the nonlinear (linear) refraction index n_2 (n_0), an effective cavity-mode volume V_{eff} , and the speed of light in vacuum c . Moreover, ω_0 is the resonance frequency of the non-spinning resonator, and the rotation leads to a Fizeau shift [S5]:

$$\omega_0 \rightarrow \omega_\pm = \omega_0 + \Delta_{\text{F}}, \quad (\text{S2})$$

with

$$\Delta_{\text{F}} = \pm \frac{nr\Omega\omega_0}{c} \left(1 - \frac{1}{n^2} - \frac{\lambda}{n} \frac{dn}{d\lambda} \right) = \pm\eta\Omega, \quad (\text{S3})$$

where $\Delta_{\text{F}} > 0$ ($\Delta_{\text{F}} < 0$) denotes the light propagating against (along) the direction of the spinning resonator, λ is the optical wavelength, n is the refractive index of the resonator, and r is the radius of the cavity. The dispersion term $dn/d\lambda$, characterizing the relativistic origin of the Sagnac effect, is relatively small ($\sim 1\%$) [S5, S6].

When the resonator is not spinning, the Fizeau drag is equal to zero, owing to the same resonance frequency of light coming from the left or right side. As implied by Eq. (S3), increasing the rotation frequency Ω results in an opposing frequency linear shift of $\eta\Omega$ (see Fig. S1) for light coming from opposite directions [S6].

S2. PHOTON BLOCKADE EFFECTS

A. Origin of photon blockade

In order to study conventional photon blockade (PB), we consider the Hamiltonian (S1) including the driving term

$$\hat{H} = \hat{H}_{\text{R}} + \hbar\xi(\hat{a}^\dagger e^{-i\omega_L t} + \hat{a}e^{i\omega_L t}), \quad (\text{S4})$$

where $\xi = \sqrt{\gamma P_{\text{in}}/(\hbar\omega_L)}$ is the driving amplitude with the cavity loss rate γ , the driving power P_{in} , and the driving frequency ω_L [S7]. In a frame rotating with the driving frequency ω_L , the Hamiltonian is transformed to

$$\hat{H}_{\text{eff}} = i\hbar \frac{d\hat{D}^\dagger}{dt} \hat{D} + \hat{D}^\dagger \hat{H} \hat{D},$$

with $\hat{D} = \exp(-i\omega_L \hat{a}^\dagger \hat{a} t)$, which leads to

$$\begin{aligned} \hat{H}_{\text{eff}} &= -\hbar\omega_L \hat{a}^\dagger \hat{a} + \hbar\omega_\pm \hat{a}^\dagger \hat{a} + \hbar U \hat{a}^\dagger \hat{a}^\dagger \hat{a} \hat{a} + \hbar\xi(\hat{a}^\dagger + \hat{a}) \\ &= \hbar(\omega_0 + \Delta_{\text{F}} - \omega_L) \hat{a}^\dagger \hat{a} + \hbar U \hat{a}^\dagger \hat{a}^\dagger \hat{a} \hat{a} + \hbar\xi(\hat{a}^\dagger + \hat{a}). \end{aligned}$$

Thus, the effective Hamiltonian of this system becomes

$$\hat{H}_{\text{eff}} = \hbar(\Delta_L + \Delta_{\text{F}}) \hat{a}^\dagger \hat{a} + \hbar U \hat{a}^\dagger \hat{a}^\dagger \hat{a} \hat{a} + \hbar\xi(\hat{a}^\dagger + \hat{a}), \quad (\text{S5})$$

where $\Delta_L = \omega_0 - \omega_L$ is the detuning between the driving field and the cavity field for the non-spinning resonator. The Hamiltonian of the isolated spinning system, i.e.,

$$H_0 = \hbar(\Delta_L + \Delta_{\text{F}}) \hat{a}^\dagger \hat{a} + \hbar U \hat{a}^\dagger \hat{a}^\dagger \hat{a} \hat{a},$$

can be expressed as

$$\begin{aligned} \hat{H}_0|n\rangle &= [\hbar\Delta_L \hat{a}^\dagger \hat{a} + \hbar\Delta_{\text{F}} \hat{a}^\dagger \hat{a} + \hbar U \hat{a}^\dagger (\hat{a} \hat{a}^\dagger - 1) \hat{a}] |n\rangle \\ &= [\hbar\Delta_L \hat{a}^\dagger \hat{a} + \hbar\Delta_{\text{F}} \hat{a}^\dagger \hat{a} + \hbar U \hat{a}^\dagger \hat{a} \hat{a}^\dagger \hat{a} - \hbar U \hat{a}^\dagger \hat{a}] |n\rangle \\ &= [\hbar\Delta_L \hat{a}^\dagger \hat{a} + \hbar(\Delta_{\text{F}} - U) \hat{a}^\dagger \hat{a} + \hbar U (\hat{a}^\dagger \hat{a})^2] |n\rangle \\ &= [n\hbar\Delta_L + n\hbar(\Delta_{\text{F}} - U) + n^2\hbar U] |n\rangle \\ &= E_n |n\rangle. \end{aligned}$$

Thus, we obtain the eigensystem for the weak-driving case,

$$\hat{H}_0|n\rangle = E_n|n\rangle, \quad (\text{S6})$$

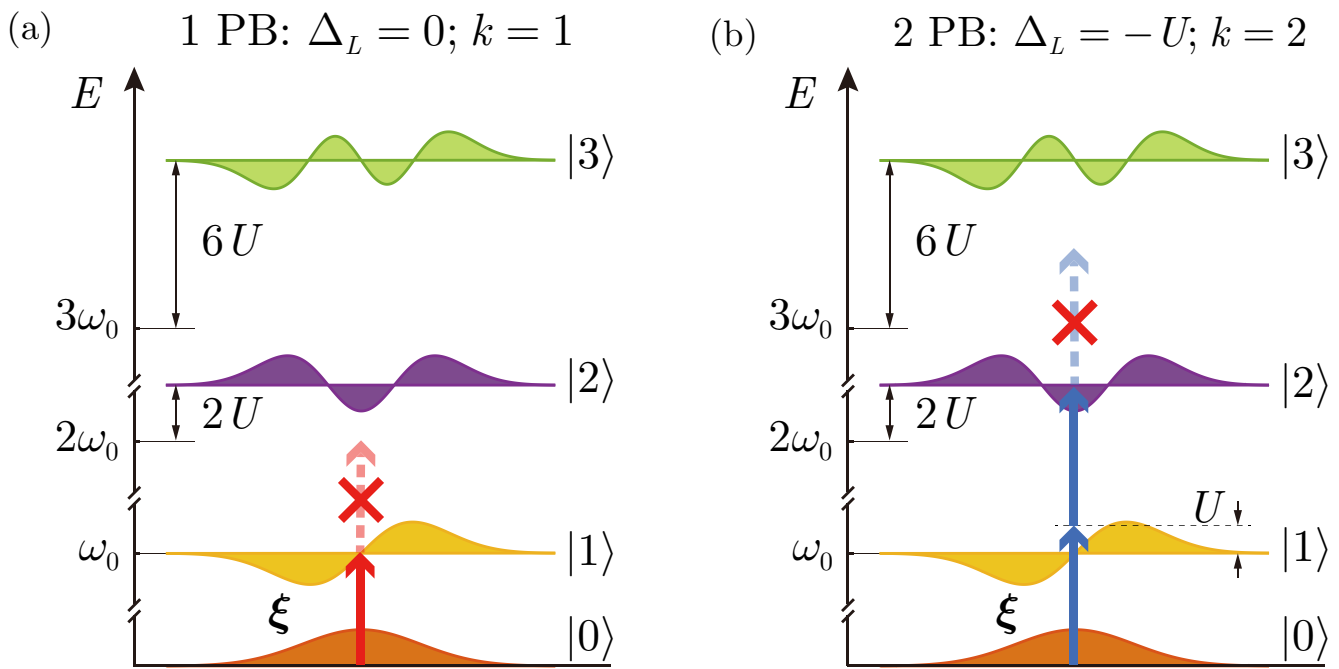


FIG. S2. Schematic energy-level diagram of the non-spinning resonator. This explains the occurrence of k -photon blockade for $\Delta_F = 0$ in terms of k -photon transitions induced by the driving field satisfying the resonance condition $\Delta_k = 0$, which corresponds to the driving-field frequency $\omega_L = \omega_0 + U(k - 1)$. Here $\hbar = 1$.

with eigenvalues

$$E_n = n\hbar\Delta_L + n\hbar\Delta_F + (n^2 - n)\hbar U = n\hbar\Delta_L + (n^2 - n)\hbar U \pm n\hbar|\Delta_F|, \quad (\text{S7})$$

where $+n\hbar|\Delta_F|$ and $-n\hbar|\Delta_F|$ denote the light propagating against ($\Delta_F > 0$) and along ($\Delta_F < 0$) the direction of the spinning resonator, respectively.

The origin of conventional n -photon blockade can be understood from the fact that due to the anharmonicity of the energy structure, i.e., the energy difference between consecutive manifolds is not constant, the Hilbert space of the system is restricted to the states containing at most n quanta. For example, when the optical resonator is non-spinning ($|\Delta_F|=0$), single-photon blockade (1PB) is illustrated in Fig. S2(a). If a coherent probe beam, tuned to ω_0 ($\Delta_L = 0$), is coupled to the system, the probe is on resonance with the $|0\rangle \rightarrow |1\rangle$ transition, but the $|1\rangle \rightarrow |2\rangle$ transition is detuned by $2\hbar U$ and is suppressed for $U > \gamma$ (where γ denotes the optical loss of the resonator). Consequently, once a photon is coupled to the system, it suppresses the probability of coupling a second photon with the same frequency. Similarly, two-photon blockade (2PB) corresponds to a two-photon resonance (2PR) for a non-spinning case, as shown in Fig. S2(b). Moreover, multi-PB corresponds to a multi-photon resonance [S4, S8–S12]. In addition to multi-PB, the energy-level diagrams of multi-photon resonances in a Kerr-type system [S4] also correspond to photon-induced tunneling (PIT) [S7, S13–S16]. This indicates that the absorption of the first photon enhances the absorption of subsequent photons [S13]. The distinction of 1PB, multi-PB, and PIT can be found by analysing higher-order correlation functions $g^{(\mu)}(0)$ with $\mu \geq 2$, as discussed below.

Due to the rotation of the resonator, different cases of nonreciprocal PB effects can be achieved. For example, Table II and Fig. S3 summarize the main results for $P_{\text{in}} = 0.3$ pW, and these are elaborated in detail later on in this Supplementary Material.

We observe that the Hamiltonian, given in Eq. (S5), can be rewritten as follows

$$\hat{H}_k = \hbar(\Delta_k + \Delta_F)\hat{a}^\dagger\hat{a} + \hbar U\hat{a}^\dagger\hat{a}(\hat{a}^\dagger\hat{a} - k) + \hbar\xi(\hat{a}^\dagger + \hat{a}), \quad (\text{S8})$$

where $\Delta_k = \Delta_L + U(k - 1)$ is the frequency mismatch for the non-spinning resonator. For convenience, we refer to k as a tuning parameter, as in Ref. [S4]. Hereafter, we analyze the resonant case of $\Delta_k = 0$, which is related to the resonant k -photon transitions in the non-spinning resonator, as shown in Fig. S2. This condition implies that the tuning parameter k is related to the Kerr nonlinearity and the driving-field and cavity frequencies as follows

$$k = -\Delta_L/U + 1. \quad (\text{S9})$$

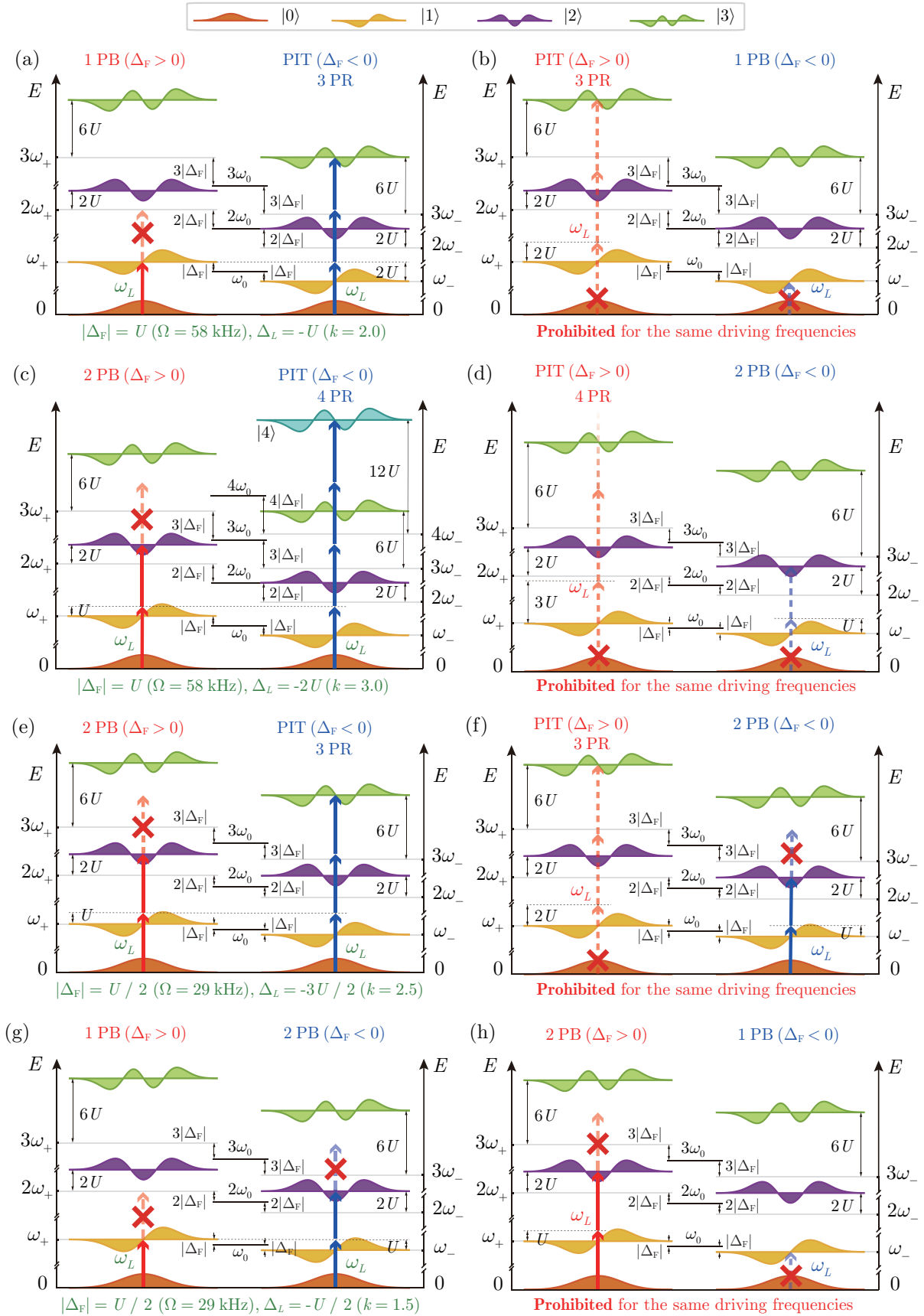


FIG. S3. Energy-level diagrams of the spinning resonator for different cases of nonreciprocal PB effects. Here, photon-induced tunneling (PIT) corresponds to an n -photon resonance (n PR), and $\hbar = 1$. All of these diagrams correspond to the cases given in Table II.

B. Criteria of photon blockade

We have studied the origin of conventional PB via the anharmonic energy-level structure. In order to describe this picture quantitatively, we apply two approaches. One is based on studying the photon-number distribution of the system [S4, S12], and the other is based on investigating the optical intensity correlations [S12, S13, S17]. Both can be experimentally measured [S12, S13, S17].

Concerning the first method, in the case of an ideal n -photon blockade, the cavity field shows the following photon-number distribution [S4]:

$$(i) \quad P(m) = 0 \quad \text{for } m > n, \quad (\text{S10a})$$

$$(ii) \quad P(n) \neq 0. \quad (\text{S10b})$$

with normalization $\sum_{m=0}^{\infty} P(m) = 1$. While the first n photons are resonantly absorbed in the system, the generation of more photons is blocked in the cavity. However, these photon-number distribution conditions are hard to achieve in an experiment, where $P(m) \neq 0$ even for $m > n$. Thus, a comparison with the Poissonian distribution was proposed by Hamsen *et al* [S12]:

$$(i) \quad P(m) < \mathcal{P}(m) \quad \text{for } m > n, \quad (\text{S11a})$$

$$(ii) \quad P(n) \geq \mathcal{P}(n). \quad (\text{S11b})$$

where $\mathcal{P}(m)$ is the Poissonian distribution

$$\mathcal{P}(m) = \frac{\langle \hat{m} \rangle^m}{m!} \exp(-\langle \hat{m} \rangle), \quad (\text{S12})$$

with the same average photon number $\langle \hat{m} \rangle$ as the cavity field. The condition, given in Eq. (S11a), indicates that the first n photons are effectively impenetrable to the following photons; while the condition, given in Eq. (S11b), indicates that the coupling of an initial photon to the system favors the coupling of the subsequent photons within the first n photons. This leads to the sub-Poissonian photon-number statistics for $(n+1)$ photons with the simultaneous super-Poissonian statistics of the first n photons. To show a relative deviation of a given photon-number distribution from the corresponding Poissonian distribution, we use the formula [S12]:

$$[P(n) - \mathcal{P}(n)]/\mathcal{P}(n). \quad (\text{S13})$$

For the second approach, correlation function $G^{(n)}(t_1, t_2, \dots, t_n)$ is the quantity measured at moments t_1, t_2, \dots, t_n in extended Hanbury Brown-Twiss experiments with n detectors. Note that $g^{(n)}$ is $G^{(n)}$ normalized by the n th power of the mean photon number. Thus, $g^{(n)}(0) \equiv \lim_{t \rightarrow \infty} G^{(n)}(t, t, \dots, t)$ is related to the probability of simultaneously measuring n photons in their steady state assuming photon detections at the same time $t = t_1 = t_2 = \dots = t_n$. The larger value of $g^{(n)}(0) > 1$, the higher probability of n -photon bunching (photon coalescence). And the smaller value of $g^{(n)}(0) < 1$, the lower probability of n -photon bunching, which corresponds to the higher probability of n -photon antibunching (photon anticorrelation). The case of $g^{(n)}(0) = 1$ is called photon unbunching, which is a typical feature of coherent light for any n . These correlation functions $G^{(n)}$ and $g^{(n)}$ are basic elements of the quantum coherence theory of Glauber [S18].”

The normalized equal-time μ th-order photon correlation is given by

$$g^{(\mu)}(0) = \sum_{m=\mu}^{\infty} \frac{m!}{(m-\mu)!} \frac{P(m)}{\langle \hat{m} \rangle^\mu} = \langle \hat{m} \rangle^{-\mu} \sum_{m=\mu}^{\infty} m(m-1)\dots(m-\mu+1)P(m) = \frac{\langle \hat{a}^{\dagger\mu} \hat{a}^\mu \rangle}{\langle \hat{a}^\dagger \hat{a} \rangle^\mu}. \quad (\text{S14})$$

In particular, the second-order photon correlation function is

$$g^{(2)}(0) = \sum_{m=2}^{\infty} m(m-1) \frac{P(m)}{\langle \hat{m} \rangle^2} = \frac{\langle \hat{m}(\hat{m}-1) \rangle}{\langle \hat{m} \rangle^2} = \frac{\langle \hat{a}^{\dagger 2} \hat{a}^2 \rangle}{\langle \hat{a}^\dagger \hat{a} \rangle^2}, \quad (\text{S15})$$

and the third-order photon correlation function is

$$g^{(3)}(0) = \sum_{m=3}^{\infty} m(m-1)(m-2) \frac{P(m)}{\langle \hat{m} \rangle^3} = \frac{\langle \hat{m}(\hat{m}-1)(\hat{m}-2) \rangle}{\langle \hat{m} \rangle^3} = \frac{\langle \hat{a}^{\dagger 3} \hat{a}^3 \rangle}{\langle \hat{a}^\dagger \hat{a} \rangle^3}. \quad (\text{S16})$$

The photon-number distribution conditions for n -photon blockade, given in Eqs. (S10a) and (S10b), can be translated into the following conditions:

$$(i) \quad g^{(n+1)}(0) = 0, \quad (\text{S17a})$$

$$(ii) \quad g^{(n)}(0) \neq 0. \quad (\text{S17b})$$

As aforementioned, these strict conditions can only be fulfilled for an ideal case. The experimentally-realizable conditions can be obtained based on Eqs. (S11a) and (S11b). Since in the weak-driving regime, the photon-number distribution fulfills the condition $P(m) \gg P(m+1)$, it is sufficient to satisfy $P(n+1) < \mathcal{P}(n+1)$ according to the condition in Eq. (S11a). Meanwhile, we can approximately express $P(n+1)$ with $g^{(n+1)}(0)$ as follows:

$$\begin{aligned} g^{(n+1)}(0) &= \sum_{m=n+1}^{\infty} \frac{m!}{(m-n-1)!} \frac{P(m)}{\langle \hat{m} \rangle^{n+1}} \approx \frac{(n+1)!}{\langle \hat{m} \rangle^{n+1}} P(n+1), \\ P(n+1) &\approx \frac{\langle \hat{m} \rangle^{n+1}}{(n+1)!} \cdot g^{(n+1)}, \end{aligned} \quad (\text{S18})$$

as the $P(m)$ have been neglected for all $m > (n+1)$. Thus, the condition, given in Eq. (S11a), reads [S12]:

$$\begin{aligned} P(n+1) &< \mathcal{P}(n+1), \\ \frac{\langle \hat{m} \rangle^{n+1}}{(n+1)!} \cdot g^{(n+1)}(0) &< \frac{\langle \hat{m} \rangle^{n+1}}{(n+1)!} \exp(-\langle \hat{m} \rangle), \\ g^{(n+1)}(0) &< \exp(-\langle \hat{m} \rangle). \end{aligned} \quad (\text{S19})$$

We can also obtain an approximate $P(n)$ using a similar method as follows:

$$\begin{aligned} g^{(n)}(0) &= \sum_{m=n}^{\infty} \frac{m!}{(m-n)!} \frac{P(m)}{\langle \hat{m} \rangle^n} \approx \frac{n!}{\langle \hat{m} \rangle^n} P(n) + \frac{(n+1)!}{\langle \hat{m} \rangle^n} P(n+1), \\ P(n) &\approx \frac{\langle \hat{m} \rangle^n}{n!} \cdot g^{(n)}(0) - (n+1)P(n+1), \\ P(n) &\approx \frac{\langle \hat{m} \rangle^n}{n!} \cdot g^{(n)}(0) - \frac{\langle \hat{m} \rangle^{n+1}}{n!} \cdot g^{(n+1)}(0). \end{aligned} \quad (\text{S20})$$

Moreover, the condition, given in Eq. (S11b), then reads:

$$\begin{aligned} P(n) &\geq \mathcal{P}(n), \\ \frac{\langle \hat{m} \rangle^n}{n!} \cdot g^{(n)}(0) - \frac{\langle \hat{m} \rangle^{n+1}}{n!} \cdot g^{(n+1)}(0) &\geq \frac{\langle \hat{m} \rangle^n}{n!} \exp(-\langle \hat{m} \rangle), \\ g^{(n)}(0) - \langle \hat{m} \rangle \cdot g^{(n+1)}(0) &\geq \exp(-\langle \hat{m} \rangle), \\ g^{(n)}(0) &\geq \exp(-\langle \hat{m} \rangle) + \langle \hat{m} \rangle \cdot g^{(n+1)}(0), \end{aligned} \quad (\text{S21})$$

i.e., the experimentally-realizable conditions, given in Eqs. (S11a) and (S11b), can be translated into the following conditions [S12]:

$$(i) \quad g^{(n+1)}(0) < \exp(-\langle \hat{m} \rangle), \quad (\text{S22a})$$

$$(ii) \quad g^{(n)}(0) \geq \exp(-\langle \hat{m} \rangle) + \langle \hat{m} \rangle \cdot g^{(n+1)}(0), \quad (\text{S22b})$$

indicating a higher-order sub-Poissonian photon-number statistics.

Moreover, PIT can be quantified by photon-number correlation functions. Table I shows that more refined criteria for PIT are sometimes applied based on higher-order correlation functions $g^{(\mu)}(0)$ with $\mu > 2$ [S16, S19]. Here, we refer to PIT if the following conditions are satisfied for $\mu \geq 2$:

$$g^{(\mu)}(0) > \exp(-\langle \hat{m} \rangle). \quad (\text{S23})$$

For simplicity, in this work, we consider these conditions only for $2 \leq \mu \leq 4$. This indicates light with higher-order super-Poissonian photon-number statistics, i.e., once, a photon is coupled in a resonator, it enhances the probabilities of more photons entering the resonator. In the few-photon regime ($\langle \hat{m} \rangle \ll 1$), these criteria become

$$g^{(\mu)}(0) > 1 \quad \text{for} \quad \mu = 2, 3, 4. \quad (\text{S24})$$

We provide a more basic criteria to identify multi-PB and PIT by using μ th-order correlation functions $g^{(\mu)}(0)$. These criteria lead to the same conclusions as those based on Eq. (S13).

TABLE I. Criteria of photon-induced tunneling (PIT) used in literature.

Reference	Criteria of PIT
Faraon <i>et al.</i> (2008) [S13]	$g^{(2)}(0)$ is a local maximum
Majumdar <i>et al.</i> (2012) [S7, S14]	$g^{(2)}(0) > 1$
Xu <i>et al.</i> (2013) [S15]	$g^{(2)}(0) > 1$ (two-photon tunneling); $g^{(3)}(0) > g^{(2)}(0) > 1$ (three-photon tunneling)
Rundquist <i>et al.</i> (2014) [S16]	$g^{(3)}(0) > g^{(2)}(0)$
Wang <i>et al.</i> (2018) [S19]	$g^{(4)}(0) > g^{(3)}(0) > g^{(2)}(0) > 1$ (phonon-induced tunneling, an analogue of PIT)

C. Single- and Multi-photon blockade

In this section, we only consider the non-spinning case ($\Delta_F=0$), while the spinning case is discussed in Sec. S4. According to criteria, given in Eqs. (S22a) and (S22b), 1PB has to fulfill the following conditions for $n = 1$:

$$(i) \quad g^{(2)}(0) < \exp(-\langle \hat{m} \rangle) \equiv f, \quad (\text{S25a})$$

$$(ii) \quad g^{(1)}(0) \geq \exp(-\langle \hat{m} \rangle) + \langle \hat{m} \rangle \cdot g^{(2)}(0) \equiv f^{(1)}. \quad (\text{S25b})$$

As expected from the intuitive picture discussed in Sec. S2 A, the strongest 1PB occurs at $\Delta_L = 0$ ($k = 1$), since the correlation functions fulfill the criteria of 1PB given in Eqs. (S25a) and (S25b) [see Fig. S4(a)]. In the weak-driving regime, $\langle \hat{m} \rangle \ll 1$ implies that $f \rightarrow 1$ and $f^{(1)} \rightarrow 1$. Then we obtain $g^{(2)}(0) < 1$, which corresponds to the usual criterion of 1PB, as known in the published literature.

As aforementioned in 1PB, the first photon blocks the entrance of a second photon, which indicates the enhancement of the single-photon probability, and also the suppression of the two- or more-photon probabilities. We can clearly see that $P(1) > \mathcal{P}(1)$, while $P(2) < \mathcal{P}(2)$ and $P(3) < \mathcal{P}(3)$ at $k = 1$ in Fig. S4(b). Moreover, 1PB can be recognized from the the deviations of the photon distribution from the standard Poissonian distribution with the same mean photon number [i.e., Eq. (S13)], as shown in Fig. S4(c-i).

At $k = 2$, we find the correlation functions fulfill $g^{(2)}(0) > g^{(3)}(0) > g^{(4)}(0) > 1$, as shown in the inset in Fig. S4(a). This shows that PIT corresponding to super-Poissonian photon-number behavior of light, which occurs at $k = 2$, since the correlation functions satisfy the conditions given in Eq. (S24). PIT can also be recognized from the photon-number distributions and the deviations given in Eq. (S13). As shown in Figs. S4(b) and S4(c-ii), we find that $P(1) < \mathcal{P}(1)$, $P(2) > \mathcal{P}(2)$, $P(3) > \mathcal{P}(3)$, and $P(4) > \mathcal{P}(4)$ at $k = 2$. This is a clear signature of PIT. Since the case for $k = 2$ corresponds to a two-photon resonance, we refer to this PIT as two-photon resonance-induced PIT.

Similarly, the 2PB has to fulfill the criteria in Eqs. (S22a) and (S22b) for $n = 2$:

$$(i) \quad g^{(3)}(0) < \exp(-\langle \hat{m} \rangle) \equiv f, \quad (\text{S26a})$$

$$(ii) \quad g^{(2)}(0) \geq \exp(-\langle \hat{m} \rangle) + \langle \hat{m} \rangle \cdot g^{(3)}(0) \equiv f^{(2)}. \quad (\text{S26b})$$

As expected from the intuitive picture discussed in Sec. S2 A, 2PB occurs at $\Delta_L = -U$ ($k = 2$), since the correlation functions fulfill the conditions of 2PB given in Eqs. (S26a) and (S26b) [see Fig. S5(a)]. We find that, at $k = 2$, $g^{(3)}(0)$ is smaller than f defined in the criterion given in Eq. (S26a), while $g^{(2)}(0)$ is greater than $f^{(2)}$ defined in the criterion given in Eq. (S26b). Here, 2PB indicates that the two-photon probability is enhanced as $P(2) > \mathcal{P}(2)$, while the other photon-number probabilities are suppressed, as shown in Figs. S5(b) and S5(c-ii). In Fig. S4, there is PIT at $k = 2$. However, in Fig. S5, there is 2PB at $k = 2$ with an enhanced input power. We note that it is necessary to properly increase the driving power to obtain a good-quality 2PB, since we need a larger average photon number. Thus, we enhance the input power from $P_{\text{in}} = 2 \text{ fW}$ (Fig. S4) to $P_{\text{in}} = 0.3 \text{ pW}$ (Fig. S5). Also, the 1PB still emerges at $k = 1$, since the second-order correlation function fulfills $g^{(2)}(0) < 1$ [see Fig. S5(a)], or only the single-photon probability is enhanced at $k = 1$ [see Figs. S5(b) and S5(c-i)].

At $k = 3$, we find the correlation functions fulfill $g^{(4)}(0) > g^{(3)}(0) > g^{(2)}(0) > 1$, as shown in the inset in Fig. S4(a). It shows PIT occurs at $k = 3$, since the correlation functions satisfy the conditions given in Eq. (S24). PIT can also be recognized from the photon-number distributions and the deviations given in Eq. (S13). As shown in Figs. S5(b) and S5(c-iii), we find that $P(1) < \mathcal{P}(1)$, $P(2) > \mathcal{P}(2)$, $P(3) > \mathcal{P}(3)$, and $P(4) > \mathcal{P}(4)$ at $k = 3$. This is a clear signature of PIT. Since the case for $k = 3$ corresponds to a three-photon resonance, we refer to this PIT as three-photon resonance-induced PIT.

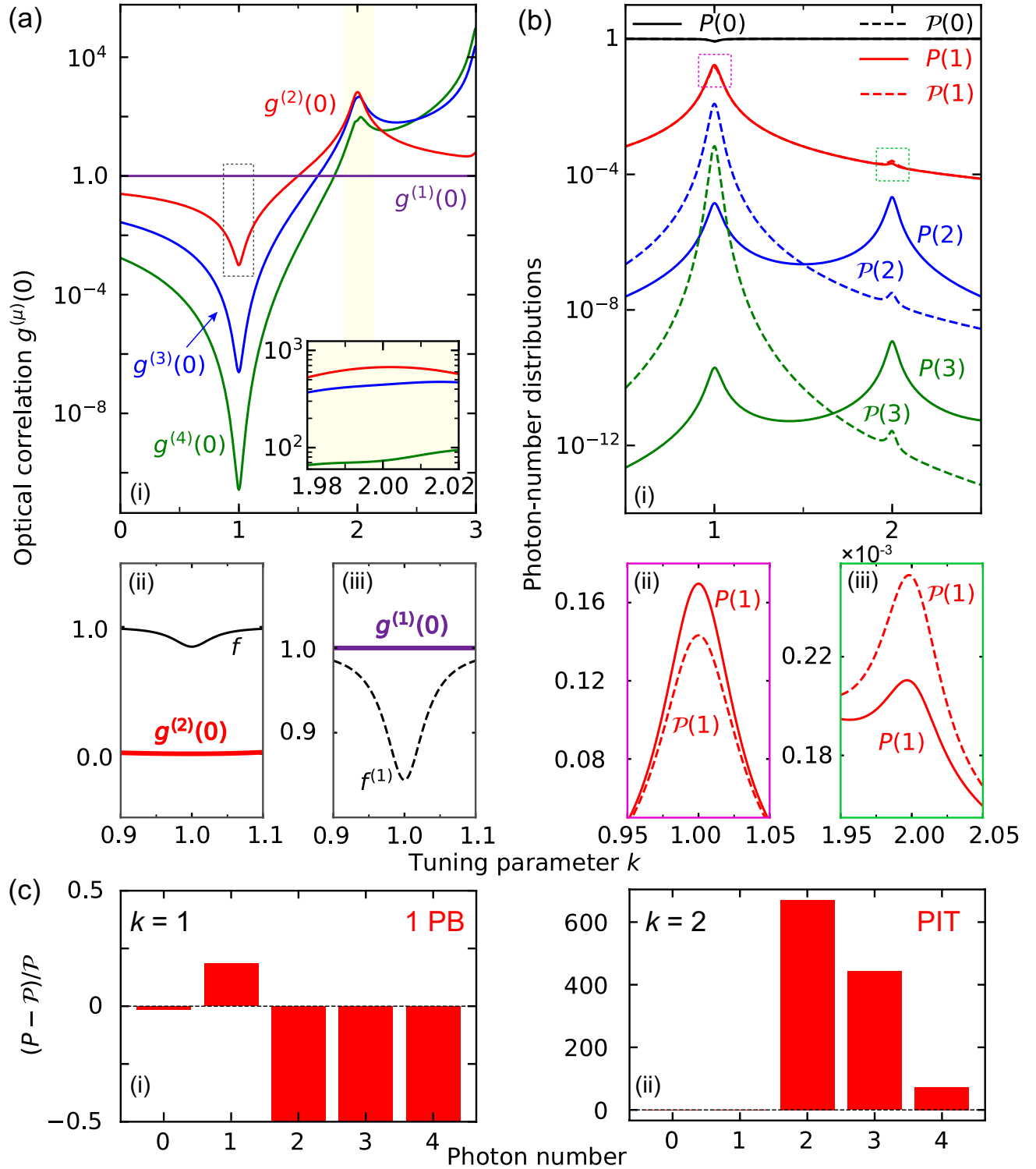


FIG. S4. (a) Correlation functions $g^{(\mu)}(0)$ versus the tuning parameter k for the non-spinning resonator ($\Delta_F = 0$). Note that 1PB emerges at $k = 1$, since (a-ii) $g^{(2)}(0) < f$ and (a-iii) $g^{(1)}(0) > f^{(1)}$ fulfill the criteria given in Eqs. (S25a) and (S25b), respectively. PIT occurs at $k = 2$, since $g^{(2)}(0) > g^{(3)}(0) > g^{(4)}(0) > 1$ [see the inset in panel (a-i)] fulfills the condition given in Eq. (S24). These 1PB and PIT can also be recognized from (b) the photon-number distributions and (c) the deviations given in Eq. (S13). At $k = 1$, (b-ii) single-photon probability is enhanced as $P(1) > \mathcal{P}(1)$, while m -photon ($m > 1$) probabilities are suppressed as $P(m) < \mathcal{P}(m)$ [see panels (b-i) and (c-i)]. These photon-number distributions fulfill the conditions given in Eqs. (S11a) and (S11b) for $n = 1$, i.e., resulting in 1PB. At $k = 2$, (b-iii) single-photon probability is suppressed as $P(1) < \mathcal{P}(1)$, while m -photon ($m > 1$) probabilities are enhanced as $P(m) > \mathcal{P}(m)$ [see panels (b-i) and (c-ii)], i.e., resulting in PIT. The parameters used here are: $\Omega = 0$, $n_2 = 3 \times 10^{-14} \text{ m}^2/\text{W}$, $n_0 = 1.4$, $V_{\text{eff}} = 150 \mu\text{m}^3$, $Q = 5 \times 10^9$, $\lambda = 1550 \text{ nm}$, $P_{\text{in}} = 2 \text{ fW}$, and $r = 30 \mu\text{m}$.

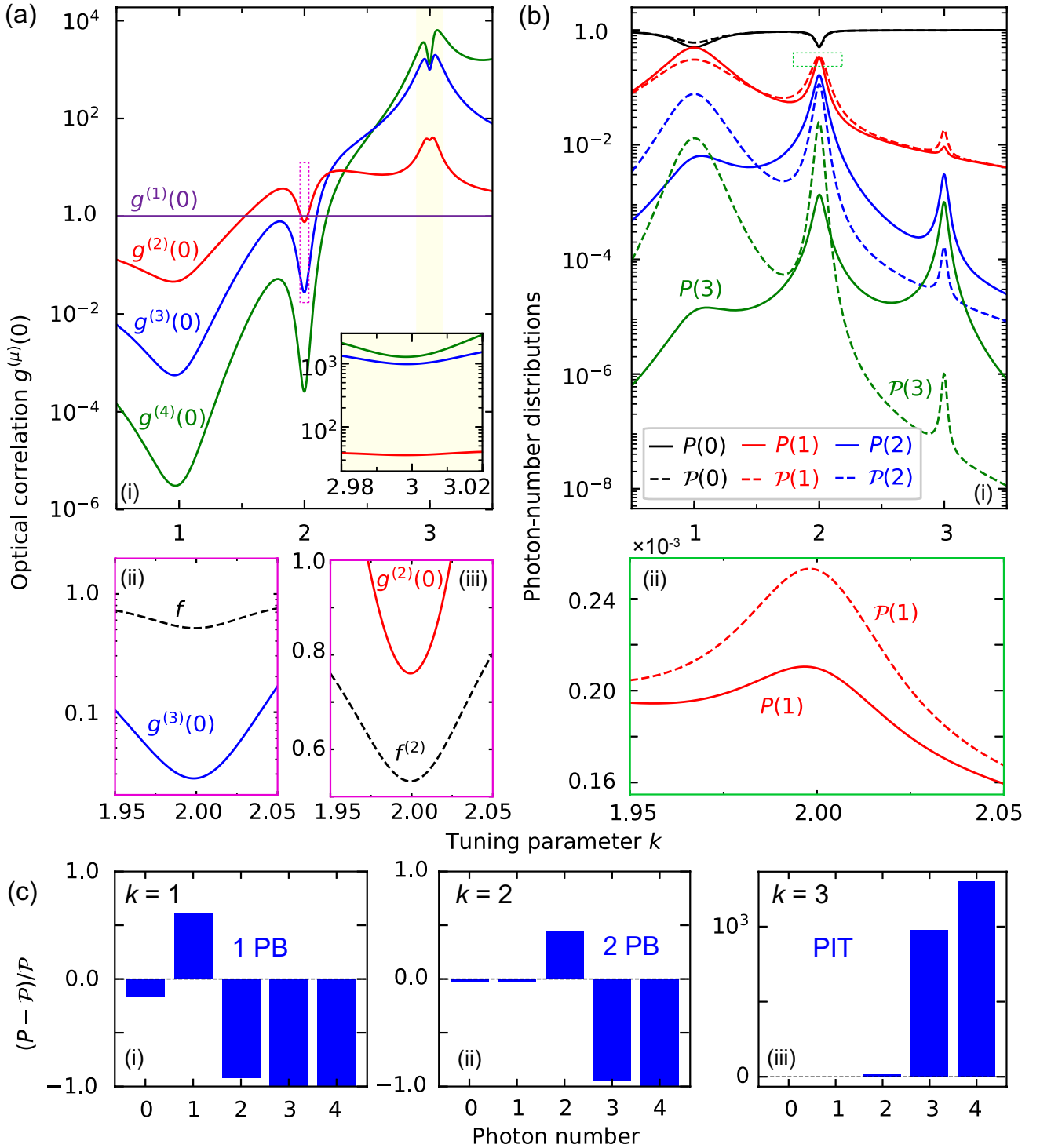


FIG. S5. (a) Correlation functions $g^{(\mu)}(0)$ versus the tuning parameter k for the non-spinning resonator ($\Delta_F = 0$). Note that 2PB occurs at $k = 2$, since (a-ii) $g^{(3)}(0) < f$ and (a-iii) $g^{(2)}(0) > f^{(2)}$ fulfill the criteria given in Eqs. (S26a) and (S26b), respectively. Also, 1PB emerges at $k = 1$, since $g^{(2)}(0) < 1$. PIT occurs at $k = 3$, since $g^{(4)}(0) > g^{(3)}(0) > g^{(2)}(0) > 1$ fulfills the conditions given in Eq. (S24) [see the inset in panel (a-i)]. These 1PB, 2PB, and PIT can also be recognized from (b) the photon-number distributions and (c) the deviations given in Eq. (S13). At $k = 1$, single-photon probability is enhanced as $P(1) > \mathcal{P}(1)$, while m -photon ($m > 1$) probabilities are suppressed as $P(m) < \mathcal{P}(m)$ [see panels (b-i) and (c-i)]. These photon-number distributions fulfill the conditions given in Eqs. (S11a) and (S11b) for $n = 1$, i.e., resulting in 1PB. At $k = 2$, only two-photon probability $P(2)$ is enhanced [see panels (b-i), (b-ii) and (c-ii)]. These photon-number distributions fulfill the conditions given in Eqs. (S11a) and (S11b) for $n = 2$, i.e., resulting in 2PB. At $k = 3$, single-photon probability is suppressed as $P(1) < \mathcal{P}(1)$, while m -photon ($m > 1$) probabilities are enhanced as $P(m) > \mathcal{P}(m)$ [see panels (b-i) and (c-ii)], i.e., resulting in PIT. Here, $P_{\text{in}} = 0.3 \text{ pW}$, and the other parameters are the same as those in Fig. S4.

In a sense, light with $g^{(3)}(0) \sim 1000$ has three-photon correlations 1000 stronger than those for coherent light. We note that the ratio of $g^{(3)}(0)/g^{(2)}(0)$ can be quite large. For example, $g^{(3)}(0)/g^{(2)}(0) \sim 100$ can be seen in Fig. S5(a). A similar prediction $g^{(3)}(0)/g^{(2)}(0) \sim 100$ has been reported in [S16]. This is possible since the mean photon number is $\langle \hat{n} \rangle \ll 1$. For example, if additionally $\langle \hat{a}^{\dagger 3} \hat{a}^3 \rangle \approx \langle \hat{a}^{\dagger 2} \hat{a}^2 \rangle$, then $g^{(3)}(0)/g^{(2)}(0) \approx 1/\langle \hat{n} \rangle \gg 1$.

S3. ANALYTIC SOLUTION OF THE OPTICAL INTENSITY CORRELATION FUNCTIONS

A. Second-order correlation function

According to the quantum trajectory method [S20], we introduce an anti-Hermitian term to the Hamiltonian in Eq. (S5) to describe the dissipation of the cavity photons. The effective non-Hermitian Hamiltonian is, thus, given by

$$\hat{H}_t = \hbar(\Delta_L + \Delta_F)\hat{a}^\dagger\hat{a} + \hbar U\hat{a}^\dagger\hat{a}^\dagger\hat{a}\hat{a} + \hbar\xi(\hat{a}^\dagger + \hat{a}) - i\hbar\frac{\gamma}{2}\hat{a}^\dagger\hat{a}, \quad (\text{S27})$$

where γ is the rate of the cavity dissipation. Then the Hamiltonian (S27) can be expressed in a *spectral representation* as

$$\begin{aligned} \hat{H}_t &= \sum_{n=0}^{\infty} \left(E_n - i\hbar\frac{\gamma}{2}n \right) |n\rangle \langle n| + \hbar\xi \sum_{n=0}^{\infty} |n\rangle \langle n| (\hat{a}^\dagger + \hat{a}) \sum_{n'=0}^{\infty} |n'\rangle \langle n'| \\ &= \sum_{n=0}^{\infty} \left(E_n - i\hbar\frac{\gamma}{2}n \right) |n\rangle \langle n| + \hbar\xi \sum_{n=0}^{\infty} \sum_{n'=0}^{\infty} |n\rangle (\langle n| \hat{a}^\dagger |n'\rangle + \langle n| \hat{a} |n'\rangle) \langle n'| \\ &= \sum_{n=0}^{\infty} \left(E_n - i\hbar\frac{\gamma}{2}n \right) |n\rangle \langle n| + \hbar\xi \sum_{n=0}^{\infty} \sum_{n'=0}^{\infty} |n\rangle (\sqrt{n'+1} \langle n|n'+1\rangle + \sqrt{n'} \langle n|n'-1\rangle) \langle n'| \\ &= \sum_{n=0}^{\infty} \left(E_n - i\hbar\frac{\gamma}{2}n \right) |n\rangle \langle n| + \hbar\xi \sum_{n=0}^{\infty} \sum_{n'=0}^{\infty} |n\rangle (\sqrt{n'+1} \delta_{n,n'+1} + \sqrt{n'} \delta_{n,n'-1}) \langle n'| \\ &= \sum_{n=0}^{\infty} \left(E_n - i\hbar\frac{\gamma}{2}n \right) |n\rangle \langle n| + \hbar\xi \sum_{n=0}^{\infty} \sum_{n'=0}^{\infty} |n\rangle (\sqrt{n'+1} \delta_{n,n'+1} + \sqrt{n'} \delta_{n',n+1}) \langle n'| \quad (\text{i}) \\ &= \sum_{n=0}^{\infty} \left(E_n - i\hbar\frac{\gamma}{2}n \right) |n\rangle \langle n| + \hbar\xi \sum_{n'=0}^{\infty} \sqrt{n'+1} |n'+1\rangle \langle n'| + \hbar\xi \sum_{n=0}^{\infty} \sqrt{n+1} |n\rangle \langle n+1| \\ &= \sum_{n=0}^{\infty} \left(E_n - i\hbar\frac{\gamma}{2}n \right) |n\rangle \langle n| + \hbar\xi \sum_{n=0}^{\infty} \sqrt{n+1} |n+1\rangle \langle n| + \hbar\xi \sum_{n=0}^{\infty} \sqrt{n+1} |n\rangle \langle n+1|, \quad (\text{ii}) \end{aligned}$$

(i) To avoid negative n , we changed the subscript of the second δ ; Also, (ii) we substituted n for n' , for convenience. Therefore, we obtain the Hamiltonian of the whole system as

$$\hat{H}_t = \sum_{n=0}^{\infty} \left(E_n - i\hbar\frac{\gamma}{2}n \right) |n\rangle \langle n| + \hbar\xi \sum_{n=0}^{\infty} \sqrt{n+1} |n+1\rangle \langle n| + \hbar\xi \sum_{n=0}^{\infty} \sqrt{n+1} |n\rangle \langle n+1|, \quad (\text{S28})$$

with eigenenergies

$$E_n = n\hbar\Delta_L + n\hbar\Delta_F + (n^2 - n)\hbar U, \quad (\text{S29})$$

where $\Delta_F > 0$ ($\Delta_F < 0$) denotes the light propagating against (along) the direction of the spinning resonator.

For the weak-driving case, we restrict to a subspace spanned by the basis states $\{|0\rangle, |1\rangle, |2\rangle\}$. Then, the Hamiltonian in Eq. (S28) becomes

$$\begin{aligned} \hat{H}_t &= E_0|0\rangle \langle 0| + \left(E_1 - i\hbar\frac{\gamma}{2} \right) |1\rangle \langle 1| + (E_2 - i\hbar\gamma)|2\rangle \langle 2| \\ &\quad + \hbar\xi\sqrt{1}|1\rangle \langle 0| + \hbar\xi\sqrt{2}|2\rangle \langle 1| + \hbar\xi\sqrt{3}|3\rangle \langle 2| \\ &\quad + \hbar\xi\sqrt{1}|0\rangle \langle 1| + \hbar\xi\sqrt{2}|1\rangle \langle 2| + \hbar\xi\sqrt{3}|2\rangle \langle 3|. \end{aligned}$$

Due to the limits of the basis states, the terms including $|3\rangle$ can be neglected. Then we have

$$\hat{H}_t = E_0|0\rangle\langle 0| + \left(E_1 - i\hbar\frac{\gamma}{2}\right)|1\rangle\langle 1| + (E_2 - i\hbar\gamma)|2\rangle\langle 2| + \hbar\xi|1\rangle\langle 0| + \hbar\xi\sqrt{2}|2\rangle\langle 1| + \hbar\xi|0\rangle\langle 1| + \hbar\xi\sqrt{2}|1\rangle\langle 2|, \quad (\text{S30})$$

where:

$$\begin{aligned} E_0 &= 0, \\ E_1 &= \hbar\Delta_L + \hbar\Delta_F, \\ E_2 &= 2\hbar\Delta_L + 2\hbar\Delta_F + 2\hbar U. \end{aligned} \quad (\text{S31})$$

In this subspace, a general state can be written as

$$|\varphi(t)\rangle = \sum_{n=0}^2 C_n(t)|n\rangle = C_0(t)|0\rangle + C_1(t)|1\rangle + C_2(t)|2\rangle. \quad (\text{S32})$$

where C_n are probability amplitudes. We substitute the Hamiltonian (S30) and the general state (S32) into the Schrödinger equation

$$i\hbar|\dot{\varphi}(t)\rangle = \hat{H}_t|\varphi(t)\rangle. \quad (\text{S33})$$

Then we have

$$i\hbar|\dot{\varphi}(t)\rangle = i\hbar\dot{C}_0(t)|0\rangle + i\hbar\dot{C}_1(t)|1\rangle + i\hbar\dot{C}_2(t)|2\rangle, \quad (\text{S34})$$

and

$$\hat{H}_t|\varphi(t)\rangle = \hat{H}_t C_0(t)|0\rangle + \hat{H}_t C_1(t)|1\rangle + \hat{H}_t C_2(t)|2\rangle, \quad (\text{S35})$$

where:

$$\hat{H}_t C_0(t)|0\rangle = (E_0|0\rangle\langle 0| + \hbar\xi|1\rangle\langle 0|)C_0(t)|0\rangle = E_0 C_0(t)|0\rangle + \hbar\xi C_0(t)|1\rangle,$$

$$\begin{aligned} \hat{H}_t C_1(t)|1\rangle &= \left[\left(E_1 - i\hbar\frac{\gamma}{2}\right)|1\rangle\langle 1| + \hbar\xi\sqrt{2}|2\rangle\langle 1| + \hbar\xi|0\rangle\langle 1| \right] C_1(t)|1\rangle \\ &= \hbar\xi C_1(t)|0\rangle + \left(E_1 - i\hbar\frac{\gamma}{2}\right) C_1(t)|1\rangle + \hbar\xi\sqrt{2} C_1(t)|2\rangle, \end{aligned}$$

$$\hat{H}_t C_2(t)|2\rangle = [(E_2 - i\hbar\gamma)|2\rangle\langle 2| + \hbar\xi\sqrt{2}|1\rangle\langle 2|] C_2(t)|2\rangle = \hbar\xi\sqrt{2} C_2(t)|1\rangle + (E_2 - i\hbar\gamma) C_2(t)|2\rangle,$$

i.e.,

$$\begin{aligned} \hat{H}_t|\varphi(t)\rangle &= [E_0 C_0(t) + \hbar\xi C_1(t)]|0\rangle + \left[\left(E_1 - i\hbar\frac{\gamma}{2}\right) C_1(t) + \hbar\xi C_0(t) + \hbar\xi\sqrt{2} C_2(t) \right] |1\rangle \\ &\quad + [(E_2 - i\hbar\gamma) C_2(t) + \hbar\xi\sqrt{2} C_1(t)]|2\rangle. \end{aligned} \quad (\text{S36})$$

By comparing the coefficients of the same basis states in Eqs. (S34) and (S36), we have:

$$\begin{aligned} i\hbar\dot{C}_0(t)|0\rangle &= [E_0 C_0(t) + \hbar\xi C_1(t)]|0\rangle, \\ i\hbar\dot{C}_1(t)|1\rangle &= \left[\left(E_1 - i\hbar\frac{\gamma}{2}\right) C_1(t) + \hbar\xi C_0(t) + \hbar\xi\sqrt{2} C_2(t) \right] |1\rangle, \\ i\hbar\dot{C}_2(t)|2\rangle &= [(E_2 - i\hbar\gamma) C_2(t) + \hbar\xi\sqrt{2} C_1(t)]|2\rangle, \end{aligned}$$

with $\nu_n = E_n/\hbar$. Then we obtain the following equations of motion for the probability amplitudes $C_n(t)$:

$$\begin{aligned} \dot{C}_0(t) &= -i\nu_0 C_0(t) - i\xi C_1(t), \\ \dot{C}_1(t) &= -i\left(\nu_1 - i\frac{\gamma}{2}\right) C_1(t) - i\xi C_0(t) - i\xi\sqrt{2} C_2(t), \\ \dot{C}_2(t) &= -i(\nu_2 - i\gamma) C_2(t) - i\xi\sqrt{2} C_1(t), \end{aligned} \quad (\text{S37})$$

where $\nu_n = E_n/\hbar$.

Weak driving means the driving strength is smaller than the cavity damping rate $\xi < \gamma$. If there is no driving field, the cavity field remains in the vacuum. When a weak-driving field is applied to the cavity, it may excite a single photon or two photons in the cavity. Thus, we have the following approximate expressions: $C_0 \sim 1$, $C_1 \sim \xi/\gamma$, and $C_2 \sim \xi^2/\gamma^2$. Then we can approximately solve the equations in Eq. (S37) using a perturbation method by discarding higher-order terms in each equation for lower-order variables. Thus, the Eq. (S37) becomes:

$$\begin{aligned}\dot{C}_0(t) &= -i\nu_0 C_0(t), \\ \dot{C}_1(t) &= -i\left(\nu_1 - i\frac{\gamma}{2}\right) C_1(t) - i\xi C_0(t), \\ \dot{C}_2(t) &= -i(\nu_2 - i\gamma)C_2(t) - i\xi\sqrt{2}C_1(t),\end{aligned}\tag{S38}$$

where $\nu_n = E_n/\hbar$.

For the initially empty cavity, the initial conditions read as: $C_0(0) = C_0(0)$, and $C_1(0) = C_2(0) = 0$. Accordingly, the solution of the zero-photon amplitude can be obtained as

$$C_0(t) = C_0(0) \exp(-i\nu_0 t).\tag{S39}$$

Hence, the equation for the single-photon amplitude in Eq. (S38) becomes

$$\dot{C}_1(t) = -i\left(\nu_1 - i\frac{\gamma}{2}\right) C_1(t) - i\xi C_0(t) \exp(-i\nu_0 t).\tag{S40}$$

To solve this equation, we introduce a slowly-varying amplitude:

$$\begin{aligned}C_1(t) &= c_1(t) \exp\left[-i\left(\nu_1 - i\frac{\gamma}{2}\right)t\right], \\ C_1(0) &= c_1(0).\end{aligned}\tag{S41}$$

Then we obtain

$$\dot{C}_1(t) = \dot{c}_1(t) \exp\left[-i\left(\nu_1 - i\frac{\gamma}{2}\right)t\right] - i\left(\nu_1 - i\frac{\gamma}{2}\right) c_1(t) \exp\left[-i\left(\nu_1 - i\frac{\gamma}{2}\right)t\right],\tag{S42}$$

and Eq. (S40) becomes:

$$\begin{aligned}\dot{c}_1(t) e^{-i(\nu_1 - i\frac{\gamma}{2})t} - i\left(\nu_1 - i\frac{\gamma}{2}\right) c_1(t) e^{-i(\nu_1 - i\frac{\gamma}{2})t} &= -i\left(\nu_1 - i\frac{\gamma}{2}\right) c_1(t) e^{-i(\nu_1 - i\frac{\gamma}{2})t} - i\xi C_0(t) e^{-i\nu_0 t}, \\ \dot{c}_1(t) &= -i\xi C_0(t) \exp\left[i\left(\nu_1 - \nu_0 - i\frac{\gamma}{2}\right)t\right].\end{aligned}\tag{S43}$$

The solution can be obtained by integrating both sides of Eq. (S43), as follows:

$$\begin{aligned}c_1(t) - c_1(0) &= -i\xi C_0(t) \int_0^t \exp\left[i\left(\nu_1 - \nu_0 - i\frac{\gamma}{2}\right)t'\right] dt', \\ c_1(t) - c_1(0) &= -i\xi \frac{C_0(t)}{i(\nu_1 - \nu_0 - i\frac{\gamma}{2})} \left\{ \exp\left[i\left(\nu_1 - \nu_0 - i\frac{\gamma}{2}\right)t\right] - 1 \right\}, \\ c_1(t) \exp\left[-i\left(\nu_1 - i\frac{\gamma}{2}\right)t\right] &= c_1(0) \exp\left[-i\left(\nu_1 - i\frac{\gamma}{2}\right)t\right] - i\xi \frac{C_0(t)}{i(\nu_1 - \nu_0 - i\frac{\gamma}{2})} \left\{ \exp(-i\nu_0 t) - \exp\left[-i\left(\nu_1 - i\frac{\gamma}{2}\right)t\right] \right\}, \\ C_1(t) &= C_1(0) \exp\left[-i\left(\nu_1 - i\frac{\gamma}{2}\right)t\right] - i\xi \frac{C_0(t)}{i(\nu_1 - \nu_0 - i\frac{\gamma}{2})} \left\{ \exp(-i\nu_0 t) - \exp\left[-i\left(\nu_1 - i\frac{\gamma}{2}\right)t\right] \right\}.\end{aligned}$$

With the initial condition $C_1(0) = 0$, we have the solution for the single-photon amplitude given by

$$C_1(t) = -i\xi \frac{C_0(t)}{i(\nu_1 - \nu_0 - i\frac{\gamma}{2})} \left\{ \exp(-i\nu_0 t) - \exp\left[-i\left(\nu_1 - i\frac{\gamma}{2}\right)t\right] \right\}.\tag{S44}$$

Consider the solution of the single-photon amplitude in Eq. (S44), the equation for the two-photon amplitude in Eq. (S38) becomes

$$\dot{C}_2(t) = -i(\nu_2 - i\gamma)C_2(t) - \sqrt{2}\xi^2 \frac{C_0(t)}{i(\nu_1 - \nu_0 - i\frac{\gamma}{2})} \left\{ \exp(-i\nu_0 t) - \exp\left[-i\left(\nu_1 - i\frac{\gamma}{2}\right)t\right] \right\}.\tag{S45}$$

To solve this equation, we introduce another slowly-varying amplitude:

$$\begin{aligned} C_2(t) &= c_2(t) \exp[-i(\nu_2 - i\gamma)t], \\ C_2(0) &= c_2(0), \end{aligned} \quad (\text{S46})$$

and obtain

$$\dot{C}_2(t) = \dot{c}_2(t) \exp[-i(\nu_2 - i\gamma)t] - i(\nu_2 - i\gamma)c_2(t) \exp[-i(\nu_2 - i\gamma)t], \quad (\text{S47})$$

then Eq. (S45) becomes:

$$\begin{aligned} \dot{c}_2(t)e^{-i(\nu_2-i\gamma)t} - i(\nu_2-i\gamma)c_2(t)e^{-i(\nu_2-i\gamma)t} &= -i(\nu_2-i\gamma)c_2(t)e^{-i(\nu_2-i\gamma)t} - \sqrt{2}\xi^2 \frac{C_0(t)}{i(\nu_1-\nu_0-i\frac{\gamma}{2})} \left[e^{-i\nu_0 t} - e^{-i(\nu_1-i\frac{\gamma}{2})t} \right], \\ \dot{c}_2(t) &= -\sqrt{2}\xi^2 \frac{C_0(t)}{i(\nu_1-\nu_0-i\frac{\gamma}{2})} \left\{ \exp[i(\nu_2-\nu_0-i\gamma)t] - \exp\left[i\left(\nu_2-\nu_1-i\frac{\gamma}{2}\right)t\right] \right\}. \end{aligned} \quad (\text{S48})$$

The solution can also be obtained by integrating both sides of Eq. (S48), as follows:

$$\begin{aligned} c_2(t) - c_2(0) &= -\sqrt{2}\xi^2 \frac{C_0(t)}{i(\nu_1-\nu_0-i\frac{\gamma}{2})} \int_0^t \left\{ \exp[i(\nu_2-\nu_0-i\gamma)t'] - \exp\left[i\left(\nu_2-\nu_1-i\frac{\gamma}{2}\right)t'\right] \right\} dt', \\ c_2(t) - c_2(0) &= -\sqrt{2}\xi^2 \frac{C_0(t)}{i(\nu_1-\nu_0-i\frac{\gamma}{2})} \left\{ \frac{\exp[i(\nu_2-\nu_0-i\gamma)t] - 1}{i(\nu_2-\nu_0-i\gamma)} - \frac{\exp\left[i\left(\nu_2-\nu_1-i\frac{\gamma}{2}\right)t\right] - 1}{i(\nu_2-\nu_1-i\frac{\gamma}{2})} \right\}, \\ c_2(t) \exp[-i(\nu_2-i\gamma)t] &= c_2(0) \exp[-i(\nu_2-i\gamma)t] - \sqrt{2}\xi^2 \frac{C_0(t)}{i(\nu_1-\nu_0-i\frac{\gamma}{2})} \cdot \frac{\exp(-i\nu_0 t) - \exp[-i(\nu_2-i\gamma)t]}{i(\nu_2-\nu_0-i\gamma)} \\ &\quad + \sqrt{2}\xi^2 \frac{C_0(t)}{i(\nu_1-\nu_0-i\frac{\gamma}{2})} \cdot \frac{\exp[-i(\nu_1-i\frac{\gamma}{2})t] - \exp[-i(\nu_2-i\gamma)t]}{i(\nu_2-\nu_1-i\frac{\gamma}{2})}, \\ C_2(t) &= C_2(0) \exp[-i(\nu_2-i\gamma)t] - \sqrt{2}\xi^2 \frac{C_0(t)}{i(\nu_1-\nu_0-i\frac{\gamma}{2})} \cdot \frac{\exp(-i\nu_0 t) - \exp[-i(\nu_2-i\gamma)t]}{i(\nu_2-\nu_0-i\gamma)} \\ &\quad + \sqrt{2}\xi^2 \frac{C_0(t)}{i(\nu_1-\nu_0-i\frac{\gamma}{2})} \cdot \frac{\exp[-i(\nu_1-i\frac{\gamma}{2})t] - \exp[-i(\nu_2-i\gamma)t]}{i(\nu_2-\nu_1-i\frac{\gamma}{2})}. \end{aligned}$$

With the initial condition $C_2(0) = 0$, we have the following solution of the two-photon amplitude

$$C_2(t) = \sqrt{2}\xi^2 \frac{C_0(t)}{(\nu_1-\nu_0-i\frac{\gamma}{2})} \left\{ \frac{\exp(-i\nu_0 t) - \exp[-i(\nu_2-i\gamma)t]}{(\nu_2-\nu_0-i\gamma)} - \frac{\exp[-i(\nu_1-i\frac{\gamma}{2})t] - \exp[-i(\nu_2-i\gamma)t]}{(\nu_2-\nu_1-i\frac{\gamma}{2})} \right\}. \quad (\text{S49})$$

Thus, for the initially empty resonator, the solutions of the equations of motion for the probability amplitudes in the equations in Eq. (S38) can be obtained as:

$$\begin{aligned} C_0(t) &= C_0(0) \exp(-i\nu_0 t), \\ C_1(t) &= -\xi \frac{C_0(t)}{(\nu_1-\nu_0-i\frac{\gamma}{2})} \left\{ \exp(-i\nu_0 t) - \exp\left[-i\left(\nu_1-i\frac{\gamma}{2}\right)t\right] \right\}, \\ C_2(t) &= \sqrt{2}\xi^2 \frac{C_0(t)}{(\nu_1-\nu_0-i\frac{\gamma}{2})} \left\{ \frac{\exp(-i\nu_0 t) - \exp[-i(\nu_2-i\gamma)t]}{(\nu_2-\nu_0-i\gamma)} - \frac{\exp[-i(\nu_1-i\frac{\gamma}{2})t] - \exp[-i(\nu_2-i\gamma)t]}{(\nu_2-\nu_1-i\frac{\gamma}{2})} \right\}, \end{aligned} \quad (\text{S50})$$

where

$$\nu_0 = 0, \quad \nu_1 = \Delta_L + \Delta_F, \quad \nu_2 = 2\Delta_L + 2\Delta_F + 2U.$$

When the initial state of the system is the vacuum state $|0\rangle$, i.e., the initial condition $C_0(0) = 1$, then the solutions

in Eq. (S50) are reduced to:

$$\begin{aligned}
C_0(t) &= 1, \\
C_1(t) &= -i\xi \frac{1}{i(\Delta_L + \Delta_F - i\frac{\gamma}{2})} \left\{ 1 - \exp \left[-i \left(\Delta_L + \Delta_F - i\frac{\gamma}{2} \right) t \right] \right\}, \\
C_2(t) &= \frac{\sqrt{2}\xi^2}{(\Delta_L + \Delta_F - i\frac{\gamma}{2})} \left\{ \frac{1 - \exp[-i(2\Delta_L + 2\Delta_F + 2U - i\gamma)t]}{(2\Delta_L + 2\Delta_F + 2U - i\gamma)} - \frac{\exp[-i(\Delta_L + \Delta_F - i\frac{\gamma}{2})t]}{(\Delta_L + \Delta_F + 2U - i\frac{\gamma}{2})} \right\} \\
&\quad + \sqrt{2}\xi^2 \cdot \frac{-\exp[i(2\Delta_L + 2\Delta_F + 2U - i\gamma)t]}{(\Delta_L + \Delta_F - i\frac{\gamma}{2})(\Delta_L + \Delta_F + 2U - i\frac{\gamma}{2})}, \tag{S51}
\end{aligned}$$

and for the infinite-time limit $\exp(-At) \rightarrow 0$ ($t \rightarrow \infty$), we have:

$$\begin{aligned}
C_0(\infty) &\equiv C_0 = 1, \\
C_1(\infty) &\equiv C_1 = \frac{-\xi}{(\Delta_L + \Delta_F - i\frac{\gamma}{2})}, \\
C_2(\infty) &\equiv C_2 = \frac{-\sqrt{2}\xi C_1}{(2\Delta_L + 2\Delta_F + 2U - i\gamma)}. \tag{S52}
\end{aligned}$$

For the state given in Eq. (S32), the infinite-time state (steady state) of the system reads as

$$|\varphi(t \rightarrow \infty)\rangle = |0\rangle + \frac{-\xi}{(\Delta_L + \Delta_F - i\frac{\gamma}{2})} |1\rangle + \frac{\sqrt{2}\xi^2}{(\Delta_L + \Delta_F - i\frac{\gamma}{2})(2\Delta_L + 2\Delta_F + 2U - i\gamma)} |2\rangle, \tag{S53}$$

and the normalization coefficient of the state is given by

$$N = 1 + |C_1|^2 + |C_2|^2, \tag{S54}$$

where:

$$|C_1|^2 = \left| \frac{\xi}{(\Delta_L + \Delta_F - i\frac{\gamma}{2})} \right|^2 = \frac{\xi^2}{(\Delta_L + \Delta_F - i\frac{\gamma}{2})(\Delta_L + \Delta_F + i\frac{\gamma}{2})} = \frac{\xi^2}{[(\Delta_L + \Delta_F)^2 + \frac{\gamma^2}{4}]}, \tag{S55}$$

$$\begin{aligned}
|C_2|^2 &= \left| \frac{\sqrt{2}\xi^2}{(\Delta_L + \Delta_F - i\frac{\gamma}{2})(2\Delta_L + 2\Delta_F + 2U - i\gamma)} \right|^2 \\
&= \frac{2\xi^4}{(\Delta_L + \Delta_F - i\frac{\gamma}{2})(\Delta_L + \Delta_F + i\frac{\gamma}{2})(2\Delta_L + 2\Delta_F + 2U - i\gamma)(2\Delta_L + 2\Delta_F + 2U + i\gamma)} \\
&= \frac{2\xi^4}{[(\Delta_L + \Delta_F)^2 + \frac{\gamma^2}{4}][4(\Delta_L + \Delta_F + U)^2 + \gamma^2]}. \tag{S56}
\end{aligned}$$

The probabilities of finding single and two photons in the cavity are, respectively, given by:

$$P_1 = \frac{|C_1|^2}{N}, \tag{S57}$$

$$P_2 = \frac{|C_2|^2}{N}. \tag{S58}$$

As mentioned in Sec. S2B, the equal-time (namely zero-time-delay) second-order correlation function can be written as

$$g^{(2)}(0) \equiv \frac{\langle \hat{a}^{\dagger 2} \hat{a}^2 \rangle}{\langle \hat{a}^{\dagger} \hat{a} \rangle^2} = \frac{\langle \hat{a}^{\dagger} \hat{a} \hat{a}^{\dagger} \hat{a} \rangle - \langle \hat{a}^{\dagger} \hat{a} \rangle^2}{\langle \hat{a}^{\dagger} \hat{a} \rangle^2}.$$

When the cavity field is in the state given in (S32), we have

$$\begin{aligned}
g^{(2)}(0) &= \frac{\sum_{n,n'=0}^2 C_n^* C_n \langle n | \hat{a}^\dagger \hat{a} \hat{a}^\dagger \hat{a} | n' \rangle - \sum_{n,n'=0}^2 C_n^* C_n \langle n | \hat{a}^\dagger \hat{a} | n' \rangle}{\left(\sum_{n,n'=0}^2 C_n^* C_n \langle n | \hat{a}^\dagger \hat{a} | n' \rangle \right)^2} \\
&= \frac{0 + |C_1|^2 + 4|C_2|^2 - (0 + |C_1|^2 + 2|C_2|^2)}{(0 + |C_1|^2 + 2|C_2|^2)^2} \\
&= \frac{N(P_1 + 4P_2 - P_1 - 2P_2)}{N^2(P_1 + 2P_2)^2} \\
&= \frac{2P_2}{N(P_1 + 2P_2)^2}.
\end{aligned}$$

In the weak-driving regime, we have the following approximate formulas: $C_0 \sim 1$, $C_1 \sim \xi/\gamma$, and $C_2 \sim \xi^2/\gamma^2$, i.e., $N \sim 1$ with $|C_2|^2 \ll |C_1|^2 \ll 1$. Hence, the second-order correlation function can be written as

$$g^{(2)}(0) \approx \frac{2P_2}{(P_1 + 2P_2)^2}. \quad (\text{S59})$$

Because $P_1 \gg P_2$, we have

$$g^{(2)}(0) \approx \frac{2P_2}{P_1^2}. \quad (\text{S60})$$

Substituting Eqs. (S57) and (S58) into Eq. (S60), we can easily obtain

$$\begin{aligned}
g^{(2)}(0) &\approx \frac{4\xi^4}{\left[(\Delta_L + \Delta_F)^2 + \frac{\gamma^2}{4} \right] [4(\Delta_L + \Delta_F + U)^2 + \gamma^2]} \cdot \frac{\left[(\Delta_L + \Delta_F)^2 + \frac{\gamma^2}{4} \right]^2}{\xi^4} \\
&= \frac{(\Delta_L + \Delta_F)^2 + \gamma^2/4}{(\Delta_L + \Delta_F + U)^2 + \gamma^2/4},
\end{aligned} \quad (\text{S61})$$

where $\Delta_F > 0$ ($\Delta_F < 0$) denotes the light propagating against (along) the direction of the spinning resonator.

Here, we focus on the non-spinning case ($\Delta_F = 0$), the rotating case is discussed in Sec. S4. Then, the second-order correlation function becomes

$$g_0^{(2)}(0) = \frac{\Delta_L^2 + \gamma^2/4}{(\Delta_L + U)^2 + \gamma^2/4}. \quad (\text{S62})$$

When the driving laser tuned to a single-photon resonance, $\Delta_L = 0$ ($k = 1$), the minimum of $g_0^{(2)}(0)$ is $g_{0\min}^{(2)} = (\gamma^2/4)/(U^2 + \gamma^2/4) = [4(U/\gamma)^2 + 1]^{-1}$. We have $g_{0\min}^{(2)} < 1$, when $U \neq 0$. The larger U/γ , the smaller is the correlation function $g_{0\min}^{(2)}$. This indicates that 1PB can be achieved. On the other hand, for the driving laser tuning to the two-photon resonance, $\Delta_L = -U$ ($k = 2$), there is $g_{0\max}^{(2)} = (U^2 + \gamma^2/4)/(\gamma^2/4) = 4(U/\gamma)^2 + 1$. We have $g_{0\max}^{(2)} > 1$ when $U \neq 0$. The larger U/γ , the larger is the correlation function $g_{0\max}^{(2)}$, which indicates a strong photon-induced tunneling caused by two-photon resonance. In Sec. S3B, we find that this conclusion is completely confirmed by our numerical results.

B. Third-order correlation function

Using a method similar to that in Sec. S3A, we calculate the third-order photon-number correlation function. For the weak-driving case, we restrict to a subspace spanned by the basis states $\{|0\rangle, |1\rangle, |2\rangle, |3\rangle\}$. Then, the Hamiltonian in Eq. (S28) becomes

$$\begin{aligned}
\hat{H}_t &= E_0|0\rangle\langle 0| + \left(E_1 - i\hbar\frac{\gamma}{2} \right) |1\rangle\langle 1| + (E_2 - i\hbar\gamma)|2\rangle\langle 2| + \left(E_3 - i\hbar\frac{3\gamma}{2} \right) |3\rangle\langle 3| \\
&\quad + \hbar\xi\sqrt{1}|1\rangle\langle 0| + \hbar\xi\sqrt{2}|2\rangle\langle 1| + \hbar\xi\sqrt{3}|3\rangle\langle 2| + \hbar\xi\sqrt{4}|4\rangle\langle 3| \\
&\quad + \hbar\xi\sqrt{1}|0\rangle\langle 1| + \hbar\xi\sqrt{2}|1\rangle\langle 2| + \hbar\xi\sqrt{3}|2\rangle\langle 3| + \hbar\xi\sqrt{4}|3\rangle\langle 4|.
\end{aligned}$$

Due to the limits of the basis states, the terms including $|4\rangle$ can be neglected. Then we have

$$\begin{aligned} \hat{H}_t = & E_0|0\rangle\langle 0| + \left(E_1 - i\hbar\frac{\gamma}{2}\right)|1\rangle\langle 1| + (E_2 - i\hbar\gamma)|2\rangle\langle 2| + \left(E_3 - i\hbar\frac{3\gamma}{2}\right)|3\rangle\langle 3| \\ & + \hbar\xi|1\rangle\langle 0| + \hbar\xi\sqrt{2}|2\rangle\langle 1| + \hbar\xi\sqrt{3}|3\rangle\langle 2| + \hbar\xi|0\rangle\langle 1| + \hbar\xi\sqrt{2}|1\rangle\langle 2| + \hbar\xi\sqrt{3}|2\rangle\langle 3|, \end{aligned} \quad (\text{S63})$$

where:

$$\begin{aligned} E_0 &= 0, \\ E_1 &= \hbar\Delta_L + \hbar\Delta_F, \\ E_2 &= 2\hbar\Delta_L + 2\hbar\Delta_F + 2\hbar U, \\ E_3 &= 3\hbar\Delta_L + 3\hbar\Delta_F + 6\hbar U. \end{aligned} \quad (\text{S64})$$

In this subspace, a general state can be written as

$$|\varphi(t)\rangle = \sum_{n=0}^3 C_n(t)|n\rangle = C_0(t)|0\rangle + C_1(t)|1\rangle + C_2(t)|2\rangle + C_3(t)|3\rangle. \quad (\text{S65})$$

where C_n are probability amplitudes. We substitute Hamiltonian (S63) and the general state (S65) into the Schrödinger equation (S33) to obtain

$$i\hbar|\dot{\varphi}(t)\rangle = i\hbar\dot{C}_0(t)|0\rangle + i\hbar\dot{C}_1(t)|1\rangle + i\hbar\dot{C}_2(t)|2\rangle + i\hbar\dot{C}_3(t)|3\rangle; \quad (\text{S66})$$

and

$$\hat{H}_t|\varphi(t)\rangle = \hat{H}_t C_0(t)|0\rangle + \hat{H}_t C_1(t)|1\rangle + \hat{H}_t C_2(t)|2\rangle + \hat{H}_t C_3(t)|3\rangle, \quad (\text{S67})$$

where:

$$\hat{H}_t C_0(t)|0\rangle = [E_0|0\rangle\langle 0| + \hbar\xi|1\rangle\langle 0|]C_0(t)|0\rangle = E_0 C_0(t)|0\rangle + \hbar\xi C_0(t)|1\rangle,$$

$$\begin{aligned} \hat{H}_t C_1(t)|1\rangle &= \left[\left(E_1 - i\hbar\frac{\gamma}{2}\right)|1\rangle\langle 1| + \hbar\xi\sqrt{2}|2\rangle\langle 1| + \hbar\xi|0\rangle\langle 1| \right] C_1(t)|1\rangle \\ &= \hbar\xi C_1(t)|0\rangle + \left(E_1 - i\hbar\frac{\gamma}{2}\right) C_1(t)|1\rangle + \hbar\xi\sqrt{2} C_1(t)|2\rangle, \end{aligned}$$

$$\begin{aligned} \hat{H}_t C_2(t)|2\rangle &= [(E_2 - i\hbar\gamma)|2\rangle\langle 2| + \hbar\xi\sqrt{2}|1\rangle\langle 2| + \hbar\xi\sqrt{3}|3\rangle\langle 2|] C_2(t)|2\rangle \\ &= \hbar\xi\sqrt{2} C_2(t)|1\rangle + (E_2 - i\hbar\gamma) C_2(t)|2\rangle + \hbar\xi\sqrt{3} C_2(t)|3\rangle, \end{aligned}$$

$$\hat{H}_t C_3(t)|3\rangle = \left[\left(E_3 - i\hbar\frac{3\gamma}{2}\right)|3\rangle\langle 3| + \hbar\xi\sqrt{3}|2\rangle\langle 3| \right] C_3(t)|3\rangle = \hbar\xi\sqrt{3} C_3(t)|2\rangle + \left(E_3 - i\hbar\frac{3\gamma}{2}\right) C_3(t)|3\rangle,$$

i.e.,

$$\begin{aligned} \hat{H}_t|\varphi(t)\rangle &= [E_0 C_0(t) + \hbar\xi C_1(t)]|0\rangle + \left[\hbar\xi C_0(t) + \left(E_1 - i\hbar\frac{\gamma}{2}\right) C_1(t) + \hbar\xi\sqrt{2} C_2(t) \right] |1\rangle \\ &+ [\hbar\xi\sqrt{2} C_1(t) + (E_2 - i\hbar\gamma) C_2(t) + \hbar\xi\sqrt{3} C_3(t)]|2\rangle + \left[\hbar\xi\sqrt{3} C_2(t) + \left(E_3 - i\hbar\frac{3\gamma}{2}\right) C_3(t) \right] |3\rangle. \end{aligned} \quad (\text{S68})$$

By comparing the coefficients of the same basis states in Eqs. (S66) and (S68), we have:

$$\begin{aligned} i\hbar\dot{C}_0(t)|0\rangle &= [E_0 C_0(t) + \hbar\xi C_1(t)]|0\rangle, \\ i\hbar\dot{C}_1(t)|1\rangle &= \left[\hbar\xi C_0(t) + \left(E_1 - i\hbar\frac{\gamma}{2}\right) C_1(t) + \hbar\xi\sqrt{2} C_2(t) \right] |1\rangle, \\ i\hbar\dot{C}_2(t)|2\rangle &= [\hbar\xi\sqrt{2} C_1(t) + (E_2 - i\hbar\gamma) C_2(t) + \hbar\xi\sqrt{3} C_3(t)]|2\rangle, \\ i\hbar\dot{C}_3(t)|3\rangle &= \left[\hbar\xi\sqrt{3} C_2(t) + \left(E_3 - i\hbar\frac{3\gamma}{2}\right) C_3(t) \right] |3\rangle, \end{aligned}$$

with $\nu_n = E_n/\hbar$. Then we obtain the following equations of motion for the probability amplitudes $C_n(t)$:

$$\begin{aligned}\dot{C}_0(t) &= -i\nu_0 C_0(t) - i\xi C_1(t), \\ \dot{C}_1(t) &= -i\xi C_0(t) - i\left(\nu_1 - i\frac{\gamma}{2}\right) C_1(t) - i\xi\sqrt{2}C_2(t), \\ \dot{C}_2(t) &= -i\xi\sqrt{2}C_1(t) - i(\nu_2 - i\gamma)C_2(t) - i\xi\sqrt{3}C_3(t), \\ \dot{C}_3(t) &= -i\xi\sqrt{3}C_2(t) - i\left(\nu_3 - i\frac{3\gamma}{2}\right) C_3(t),\end{aligned}\tag{S69}$$

where $\nu_n = E_n/\hbar$.

Similarly, due to the weak-driving case, we have the following approximate formulas: $C_0 \sim 1$, $C_1 \sim \xi/\gamma$, $C_2 \sim \xi^2/\gamma^2$, and $C_3 \sim \xi^3/\gamma^3$. Then we can approximately solve the equations in Eq. (S69) using a perturbation method by discarding higher-order terms in each equation for lower-order variables. Thus, the Eq. (S69) becomes:

$$\begin{aligned}\dot{C}_0(t) &= -i\nu_0 C_0(t), \\ \dot{C}_1(t) &= -i\left(\nu_1 - i\frac{\gamma}{2}\right) C_1(t) - i\xi C_0(t), \\ \dot{C}_2(t) &= -i(\nu_2 - i\gamma)C_2(t) - i\xi\sqrt{2}C_1(t), \\ \dot{C}_3(t) &= -i\left(\nu_3 - i\frac{3\gamma}{2}\right) C_3(t) - i\xi\sqrt{3}C_2(t),\end{aligned}\tag{S70}$$

where $\nu_n = E_n/\hbar$.

For an initially empty cavity, the initial conditions read as: $C_0(0) = C_0(0)$, and $C_1(0) = C_2(0) = C_3(0) = 0$. Then, the solution of the zero-photon amplitude can be obtained as

$$C_0(t) = C_0(0) \exp(-i\nu_0 t).\tag{S71}$$

Hence, the equation for the single-photon amplitude in Eq. (S70) becomes

$$\dot{C}_1(t) = -i\left(\nu_1 - i\frac{\gamma}{2}\right) C_1(t) - i\xi C_0(0) \exp(-i\nu_0 t).\tag{S72}$$

To solve this equation, we introduce a slowly-varying amplitude:

$$\begin{aligned}C_1(t) &= c_1(t) \exp\left[-i\left(\nu_1 - i\frac{\gamma}{2}\right)t\right], \\ C_1(0) &= c_1(0),\end{aligned}\tag{S73}$$

then we obtain

$$\dot{C}_1(t) = \dot{c}_1(t) \exp\left[-i\left(\nu_1 - i\frac{\gamma}{2}\right)t\right] - i\left(\nu_1 - i\frac{\gamma}{2}\right) c_1(t) \exp\left[-i\left(\nu_1 - i\frac{\gamma}{2}\right)t\right],\tag{S74}$$

and Eq. (S72) becomes:

$$\begin{aligned}\dot{c}_1(t) e^{-i(\nu_1 - i\frac{\gamma}{2})t} - i\left(\nu_1 - i\frac{\gamma}{2}\right) c_1(t) e^{-i(\nu_1 - i\frac{\gamma}{2})t} &= -i\left(\nu_1 - i\frac{\gamma}{2}\right) c_1(t) e^{-i(\nu_1 - i\frac{\gamma}{2})t} - i\xi C_0(0) e^{-i\nu_0 t}, \\ \dot{c}_1(t) &= -i\xi C_0(0) \exp\left[i\left(\nu_1 - \nu_0 - i\frac{\gamma}{2}\right)t\right].\end{aligned}\tag{S75}$$

The solution can be obtained by integrating both sides of Eq. (S75), as follows:

$$\begin{aligned}c_1(t) - c_1(0) &= -i\xi C_0(0) \int_0^t \exp\left[i\left(\nu_1 - \nu_0 - i\frac{\gamma}{2}\right)t'\right] dt', \\ c_1(t) - c_1(0) &= -i\xi \frac{C_0(0)}{i(\nu_1 - \nu_0 - i\frac{\gamma}{2})} \left\{ \exp\left[i\left(\nu_1 - \nu_0 - i\frac{\gamma}{2}\right)t\right] - 1 \right\}, \\ c_1(t) \exp\left[-i\left(\nu_1 - i\frac{\gamma}{2}\right)t\right] &= c_1(0) \exp\left[-i\left(\nu_1 - i\frac{\gamma}{2}\right)t\right] - i\xi \frac{C_0(0)}{i(\nu_1 - \nu_0 - i\frac{\gamma}{2})} \left\{ \exp(-i\nu_0 t) - \exp\left[-i\left(\nu_1 - i\frac{\gamma}{2}\right)t\right] \right\}, \\ C_1(t) &= C_1(0) \exp\left[-i\left(\nu_1 - i\frac{\gamma}{2}\right)t\right] - i\xi \frac{C_0(0)}{i(\nu_1 - \nu_0 - i\frac{\gamma}{2})} \left\{ \exp(-i\nu_0 t) - \exp\left[-i\left(\nu_1 - i\frac{\gamma}{2}\right)t\right] \right\}.\end{aligned}$$

With the initial condition $C_1(0) = 0$, we have the solution for the single-photon amplitude given by

$$C_1(t) = -i\xi \frac{C_0(0)}{i(\nu_1 - \nu_0 - i\frac{\gamma}{2})} \left\{ \exp(-i\nu_0 t) - \exp\left[-i\left(\nu_1 - i\frac{\gamma}{2}\right)t\right] \right\}. \quad (\text{S76})$$

Consider the solution of the single-photon amplitude in Eq. (S76), the equation for the two-photon amplitude in Eq. (S70) becomes

$$\dot{C}_2(t) = -i(\nu_2 - i\gamma)C_2(t) - \sqrt{2}\xi^2 \frac{C_0(0)}{i(\nu_1 - \nu_0 - i\frac{\gamma}{2})} \left\{ \exp(-i\nu_0 t) - \exp\left[-i\left(\nu_1 - i\frac{\gamma}{2}\right)t\right] \right\}. \quad (\text{S77})$$

To solve this equation, we introduce another slowly-varying amplitude:

$$\begin{aligned} C_2(t) &= c_2(t) \exp[-i(\nu_2 - i\gamma)t], \\ C_2(0) &= c_2(0), \end{aligned} \quad (\text{S78})$$

and obtain

$$\dot{C}_2(t) = \dot{c}_2(t) \exp[-i(\nu_2 - i\gamma)t] - i(\nu_2 - i\gamma)c_2(t) \exp[-i(\nu_2 - i\gamma)t], \quad (\text{S79})$$

then Eq. (S77) becomes:

$$\begin{aligned} \dot{c}_2(t) e^{-i(\nu_2 - i\gamma)t} - i(\nu_2 - i\gamma)c_2(t) e^{-i(\nu_2 - i\gamma)t} &= -i(\nu_2 - i\gamma)c_2(t) e^{-i(\nu_2 - i\gamma)t} - \sqrt{2}\xi^2 \frac{C_0(0)}{i(\nu_1 - \nu_0 - i\frac{\gamma}{2})} \left[e^{-i\nu_0 t} - e^{-i(\nu_1 - i\frac{\gamma}{2})t} \right], \\ \dot{c}_2(t) &= -\sqrt{2}\xi^2 \frac{C_0(0)}{i(\nu_1 - \nu_0 - i\frac{\gamma}{2})} \left\{ \exp[i(\nu_2 - \nu_0 - i\gamma)t] - \exp\left[i\left(\nu_2 - \nu_1 - i\frac{\gamma}{2}\right)t\right] \right\}. \end{aligned} \quad (\text{S80})$$

The solution can also be obtained by integrating both sides of Eq. (S80), as follows:

$$\begin{aligned} c_2(t) - c_2(0) &= -\sqrt{2}\xi^2 \frac{C_0(0)}{i(\nu_1 - \nu_0 - i\frac{\gamma}{2})} \int_0^t \left\{ \exp[i(\nu_2 - \nu_0 - i\gamma)t'] - \exp\left[i\left(\nu_2 - \nu_1 - i\frac{\gamma}{2}\right)t'\right] \right\} dt', \\ c_2(t) - c_2(0) &= -\sqrt{2}\xi^2 \frac{C_0(0)}{i(\nu_1 - \nu_0 - i\frac{\gamma}{2})} \left\{ \frac{\exp[i(\nu_2 - \nu_0 - i\gamma)t] - 1}{i(\nu_2 - \nu_0 - i\gamma)} - \frac{\exp\left[i\left(\nu_2 - \nu_1 - i\frac{\gamma}{2}\right)t\right] - 1}{i\left(\nu_2 - \nu_1 - i\frac{\gamma}{2}\right)} \right\}, \\ c_2(t) \exp[-i(\nu_2 - i\gamma)t] &= c_2(0) \exp[-i(\nu_2 - i\gamma)t] - \sqrt{2}\xi^2 \frac{C_0(0)}{i(\nu_1 - \nu_0 - i\frac{\gamma}{2})} \cdot \frac{\exp(-i\nu_0 t) - \exp[-i(\nu_2 - i\gamma)t]}{i(\nu_2 - \nu_0 - i\gamma)} \\ &\quad + \sqrt{2}\xi^2 \frac{C_0(0)}{i(\nu_1 - \nu_0 - i\frac{\gamma}{2})} \cdot \frac{\exp\left[-i\left(\nu_1 - i\frac{\gamma}{2}\right)t\right] - \exp[-i(\nu_2 - i\gamma)t]}{i\left(\nu_2 - \nu_1 - i\frac{\gamma}{2}\right)}, \\ C_2(t) &= C_2(0) \exp[-i(\nu_2 - i\gamma)t] - \sqrt{2}\xi^2 \frac{C_0(0)}{i(\nu_1 - \nu_0 - i\frac{\gamma}{2})} \cdot \frac{\exp(-i\nu_0 t) - \exp[-i(\nu_2 - i\gamma)t]}{i(\nu_2 - \nu_0 - i\gamma)} \\ &\quad + \sqrt{2}\xi^2 \frac{C_0(0)}{i(\nu_1 - \nu_0 - i\frac{\gamma}{2})} \cdot \frac{\exp\left[-i\left(\nu_1 - i\frac{\gamma}{2}\right)t\right] - \exp[-i(\nu_2 - i\gamma)t]}{i\left(\nu_2 - \nu_1 - i\frac{\gamma}{2}\right)}. \end{aligned}$$

With the initial condition $C_2(0) = 0$, we have the following solution of the two-photon amplitude

$$C_2(t) = \sqrt{2}\xi^2 \frac{C_0(0)}{(\nu_1 - \nu_0 - i\frac{\gamma}{2})} \left\{ \frac{\exp(-i\nu_0 t) - \exp[-i(\nu_2 - i\gamma)t]}{(\nu_2 - \nu_0 - i\gamma)} - \frac{\exp\left[-i\left(\nu_1 - i\frac{\gamma}{2}\right)t\right] - \exp[-i(\nu_2 - i\gamma)t]}{(\nu_2 - \nu_1 - i\frac{\gamma}{2})} \right\}. \quad (\text{S81})$$

Consider the solution of the two-photon amplitude in Eq. (S81), the equation for the three-photon amplitude in Eq. (S70) becomes

$$\begin{aligned} \dot{C}_3(t) &= -i\left(\nu_3 - i\frac{3\gamma}{2}\right) C_3(t) + \sqrt{6}\xi^3 C_0(0) \frac{\exp(-i\nu_0 t) - \exp[-i(\nu_2 - i\gamma)t]}{i(\nu_1 - \nu_0 - i\frac{\gamma}{2})(\nu_2 - \nu_0 - i\gamma)} \\ &\quad - \sqrt{6}\xi^3 C_0(0) \frac{\exp\left[-i\left(\nu_1 - i\frac{\gamma}{2}\right)t\right] - \exp[-i(\nu_2 - i\gamma)t]}{i(\nu_1 - \nu_0 - i\frac{\gamma}{2})(\nu_2 - \nu_1 - i\frac{\gamma}{2})}. \end{aligned} \quad (\text{S82})$$

To solve this equation, we introduce the slowly-varying amplitude:

$$\begin{aligned} C_3(t) &= c_3(t) \exp \left[-i \left(\nu_3 - i \frac{3\gamma}{2} \right) t \right], \\ C_3(0) &= c_3(0), \end{aligned} \quad (\text{S83})$$

and obtain

$$\dot{C}_3(t) = \dot{c}_3(t) \exp \left[-i \left(\nu_3 - i \frac{3\gamma}{2} \right) t \right] - i \left(\nu_3 - i \frac{3\gamma}{2} \right) c_3(t) \exp \left[-i \left(\nu_3 - i \frac{3\gamma}{2} \right) t \right], \quad (\text{S84})$$

then Eq. (S82) becomes:

$$\begin{aligned} \dot{c}_3(t) e^{-i(\nu_3 - i\frac{3\gamma}{2})t} - i \left(\nu_3 - i \frac{3\gamma}{2} \right) c_3(t) e^{-i(\nu_3 - i\frac{3\gamma}{2})t} &= -i \left(\nu_3 - i \frac{3\gamma}{2} \right) C_3(t) + \sqrt{6}\xi^3 C_0(0) \frac{e^{-i\nu_0 t} - e^{-i(\nu_2 - i\gamma)t}}{i(\nu_1 - \nu_0 - i\frac{\gamma}{2})(\nu_2 - \nu_0 - i\gamma)} \\ &\quad - \sqrt{6}\xi^3 C_0(0) \frac{e^{-i(\nu_1 - i\frac{\gamma}{2})t} - e^{-i(\nu_2 - i\gamma)t}}{i(\nu_1 - \nu_0 - i\frac{\gamma}{2})(\nu_2 - \nu_1 - i\frac{\gamma}{2})}, \\ \dot{c}_3(t) &= \sqrt{6}\xi^3 C_0(0) \frac{\exp \left[i(\nu_3 - \nu_0 - i\frac{3\gamma}{2})t \right] - \exp \left[i(\nu_3 - \nu_2 - i\frac{\gamma}{2})t \right]}{i(\nu_1 - \nu_0 - i\frac{\gamma}{2})(\nu_2 - \nu_0 - i\gamma)} \\ &\quad - \sqrt{6}\xi^3 C_0(0) \frac{\exp \left[i(\nu_3 - \nu_1 - i\gamma)t \right] - \exp \left[-i(\nu_3 - \nu_2 - i\frac{\gamma}{2})t \right]}{i(\nu_1 - \nu_0 - i\frac{\gamma}{2})(\nu_2 - \nu_1 - i\frac{\gamma}{2})}. \end{aligned} \quad (\text{S85})$$

The solution can also be obtained by integrating both sides of Eq. (S85), as follows:

$$\begin{aligned} c_3(t) - c_3(0) &= \sqrt{6}\xi^3 \frac{C_0(0)}{i(\nu_1 - \nu_0 - i\frac{\gamma}{2})(\nu_2 - \nu_0 - i\gamma)} \int_0^t \left\{ \exp \left[i(\nu_3 - \nu_0 - i\frac{3\gamma}{2})t' \right] - \exp \left[i(\nu_3 - \nu_2 - i\frac{\gamma}{2})t' \right] \right\} dt' \\ &\quad - \sqrt{6}\xi^3 \frac{C_0(0)}{i(\nu_1 - \nu_0 - i\frac{\gamma}{2})(\nu_2 - \nu_1 - i\frac{\gamma}{2})} \int_0^t \left\{ \exp \left[i(\nu_3 - \nu_1 - i\gamma)t' \right] - \exp \left[-i(\nu_3 - \nu_2 - i\frac{\gamma}{2})t' \right] \right\} dt' \\ &= \sqrt{6}\xi^3 \frac{C_0(0)}{i(\nu_1 - \nu_0 - i\frac{\gamma}{2})(\nu_2 - \nu_0 - i\gamma)} \left\{ \frac{\exp \left[i(\nu_3 - \nu_0 - i\frac{3\gamma}{2})t \right] - 1}{i(\nu_3 - \nu_0 - i\frac{3\gamma}{2})} - \frac{\exp \left[i(\nu_3 - \nu_2 - i\frac{\gamma}{2})t \right] - 1}{i(\nu_3 - \nu_2 - i\frac{\gamma}{2})} \right\} \\ &\quad - \sqrt{6}\xi^3 \frac{C_0(0)}{i(\nu_1 - \nu_0 - i\frac{\gamma}{2})(\nu_2 - \nu_1 - i\frac{\gamma}{2})} \left\{ \frac{\exp \left[i(\nu_3 - \nu_1 - i\gamma)t \right] - 1}{i(\nu_3 - \nu_1 - i\gamma)} - \frac{\exp \left[i(\nu_3 - \nu_2 - i\frac{\gamma}{2})t \right] - 1}{i(\nu_3 - \nu_2 - i\frac{\gamma}{2})} \right\}, \\ c_3(t) \exp \left[-i \left(\nu_3 - i \frac{3\gamma}{2} \right) t \right] &= c_3(0) \exp \left[-i \left(\nu_3 - i \frac{3\gamma}{2} \right) t \right] - \sqrt{6}\xi^3 \frac{C_0(0)}{(\nu_1 - \nu_0 - i\frac{\gamma}{2})(\nu_2 - \nu_0 - i\gamma)(\nu_3 - \nu_0 - i\frac{3\gamma}{2})} \left\{ \exp(-i\nu_0 t) - \exp \left[-i \left(\nu_3 - i \frac{3\gamma}{2} \right) t \right] \right\} \\ &\quad + \sqrt{6}\xi^3 \frac{C_0(0)}{(\nu_1 - \nu_0 - i\frac{\gamma}{2})(\nu_2 - \nu_0 - i\gamma)(\nu_3 - \nu_2 - i\frac{\gamma}{2})} \left\{ \exp \left[-i(\nu_2 - i\gamma)t \right] - \exp \left[-i \left(\nu_3 - i \frac{3\gamma}{2} \right) t \right] \right\} \\ &\quad + \sqrt{6}\xi^3 \frac{C_0(0)}{(\nu_1 - \nu_0 - i\frac{\gamma}{2})(\nu_2 - \nu_1 - i\frac{\gamma}{2})(\nu_3 - \nu_1 - i\gamma)} \left\{ \exp \left[-i \left(\nu_1 - i \frac{\gamma}{2} \right) t \right] - \exp \left[-i \left(\nu_3 - i \frac{3\gamma}{2} \right) t \right] \right\} \\ &\quad - \sqrt{6}\xi^3 \frac{C_0(0)}{(\nu_1 - \nu_0 - i\frac{\gamma}{2})(\nu_2 - \nu_1 - i\frac{\gamma}{2})(\nu_3 - \nu_2 - i\frac{\gamma}{2})} \left\{ \exp \left[-i(\nu_2 - i\gamma)t \right] - \exp \left[-i \left(\nu_3 - i \frac{3\gamma}{2} \right) t \right] \right\}, \\ C_3(t) &= C_3(0) \exp \left[-i \left(\nu_3 - i \frac{3\gamma}{2} \right) t \right] - \sqrt{6}\xi^3 \frac{C_0(0)}{(\nu_1 - \nu_0 - i\frac{\gamma}{2})(\nu_2 - \nu_0 - i\gamma)(\nu_3 - \nu_0 - i\frac{3\gamma}{2})} \left\{ \exp(-i\nu_0 t) - \exp \left[-i \left(\nu_3 - i \frac{3\gamma}{2} \right) t \right] \right\} \\ &\quad + \sqrt{6}\xi^3 \frac{C_0(0)}{(\nu_1 - \nu_0 - i\frac{\gamma}{2})(\nu_2 - \nu_0 - i\gamma)(\nu_3 - \nu_2 - i\frac{\gamma}{2})} \left\{ \exp \left[-i(\nu_2 - i\gamma)t \right] - \exp \left[-i \left(\nu_3 - i \frac{3\gamma}{2} \right) t \right] \right\} \\ &\quad + \sqrt{6}\xi^3 \frac{C_0(0)}{(\nu_1 - \nu_0 - i\frac{\gamma}{2})(\nu_2 - \nu_1 - i\frac{\gamma}{2})(\nu_3 - \nu_1 - i\gamma)} \left\{ \exp \left[-i \left(\nu_1 - i \frac{\gamma}{2} \right) t \right] - \exp \left[-i \left(\nu_3 - i \frac{3\gamma}{2} \right) t \right] \right\} \\ &\quad - \sqrt{6}\xi^3 \frac{C_0(0)}{(\nu_1 - \nu_0 - i\frac{\gamma}{2})(\nu_2 - \nu_1 - i\frac{\gamma}{2})(\nu_3 - \nu_2 - i\frac{\gamma}{2})} \left\{ \exp \left[-i(\nu_2 - i\gamma)t \right] - \exp \left[-i \left(\nu_3 - i \frac{3\gamma}{2} \right) t \right] \right\}. \end{aligned}$$

With the initial condition $C_3(0) = 0$, we have the following solution of the three-photon amplitude

$$\begin{aligned}
C_3(t) = & -\sqrt{6}\xi^3 \frac{C_0(0) \{ \exp(-i\nu_0 t) - \exp[-i(\nu_3 - i\frac{3\gamma}{2})t] \}}{(\nu_1 - \nu_0 - i\frac{\gamma}{2})(\nu_2 - \nu_0 - i\gamma)(\nu_3 - \nu_0 - i\frac{3\gamma}{2})} \\
& + \sqrt{6}\xi^3 \frac{C_0(0) \{ \exp[-i(\nu_2 - i\gamma)t] - \exp[-i(\nu_3 - i\frac{3\gamma}{2})t] \}}{(\nu_1 - \nu_0 - i\frac{\gamma}{2})(\nu_2 - \nu_0 - i\gamma)(\nu_3 - \nu_2 - i\frac{\gamma}{2})} \\
& + \sqrt{6}\xi^3 \frac{C_0(0) \{ \exp[-i(\nu_1 - i\frac{\gamma}{2})t] - \exp[-i(\nu_3 - i\frac{3\gamma}{2})t] \}}{(\nu_1 - \nu_0 - i\frac{\gamma}{2})(\nu_2 - \nu_1 - i\frac{\gamma}{2})(\nu_3 - \nu_1 - i\gamma)} \\
& - \sqrt{6}\xi^3 \frac{C_0(0) \{ \exp[-i(\nu_2 - i\gamma)t] - \exp[-i(\nu_3 - i\frac{3\gamma}{2})t] \}}{(\nu_1 - \nu_0 - i\frac{\gamma}{2})(\nu_2 - \nu_1 - i\frac{\gamma}{2})(\nu_3 - \nu_2 - i\frac{\gamma}{2})}.
\end{aligned} \tag{S86}$$

Thus, for the initially empty resonator, the solutions of the equations of motion for the probability amplitudes in the equations in Eq. (S70) can be obtained as:

$$\begin{aligned}
C_0(t) &= C_0(0) \exp(-i\nu_0 t), \\
C_1(t) &= -\xi \frac{C_0(0)}{(\nu_1 - \nu_0 - i\frac{\gamma}{2})} \left\{ \exp(-i\nu_0 t) - \exp\left[-i\left(\nu_1 - i\frac{\gamma}{2}\right)t\right] \right\}, \\
C_2(t) &= \sqrt{2}\xi^2 \frac{C_0(0)}{(\nu_1 - \nu_0 - i\frac{\gamma}{2})} \left\{ \frac{\exp(-i\nu_0 t) - \exp[-i(\nu_2 - i\gamma)t]}{(\nu_2 - \nu_0 - i\gamma)} - \frac{\exp[-i(\nu_1 - i\frac{\gamma}{2})t] - \exp[-i(\nu_2 - i\gamma)t]}{(\nu_2 - \nu_1 - i\frac{\gamma}{2})} \right\}, \\
C_3(t) &= -\sqrt{6}\xi^3 \frac{C_0(0) \{ \exp(-i\nu_0 t) - \exp[-i(\nu_3 - i\frac{3\gamma}{2})t] \}}{(\nu_1 - \nu_0 - i\frac{\gamma}{2})(\nu_2 - \nu_0 - i\gamma)(\nu_3 - \nu_0 - i\frac{3\gamma}{2})} \\
& + \sqrt{6}\xi^3 \frac{C_0(0) \{ \exp[-i(\nu_2 - i\gamma)t] - \exp[-i(\nu_3 - i\frac{3\gamma}{2})t] \}}{(\nu_1 - \nu_0 - i\frac{\gamma}{2})(\nu_2 - \nu_0 - i\gamma)(\nu_3 - \nu_2 - i\frac{\gamma}{2})} \\
& + \sqrt{6}\xi^3 \frac{C_0(0) \{ \exp[-i(\nu_1 - i\frac{\gamma}{2})t] - \exp[-i(\nu_3 - i\frac{3\gamma}{2})t] \}}{(\nu_1 - \nu_0 - i\frac{\gamma}{2})(\nu_2 - \nu_1 - i\frac{\gamma}{2})(\nu_3 - \nu_1 - i\gamma)} \\
& - \sqrt{6}\xi^3 \frac{C_0(0) \{ \exp[-i(\nu_2 - i\gamma)t] - \exp[-i(\nu_3 - i\frac{3\gamma}{2})t] \}}{(\nu_1 - \nu_0 - i\frac{\gamma}{2})(\nu_2 - \nu_1 - i\frac{\gamma}{2})(\nu_3 - \nu_2 - i\frac{\gamma}{2})},
\end{aligned} \tag{S87}$$

where

$$\nu_0 = 0, \quad \nu_1 = \Delta_L + \Delta_F, \quad \nu_2 = 2\Delta_L + 2\Delta_F + 2U, \quad \nu_3 = 3\Delta_L + 3\Delta_F + 6U.$$

When the initial state of the system is the vacuum state $|0\rangle$, i.e., the initial condition $C_0(0) = 1$, the solutions in Eq. (S87) are reduced to:

$$\begin{aligned}
C_0(t) &= 1, \\
C_1(t) &= -\xi \frac{1}{(\Delta_L + \Delta_F - i\frac{\gamma}{2})} \left\{ 1 - \exp\left[-i\left(\Delta_L + \Delta_F - i\frac{\gamma}{2}\right)t\right] \right\}, \\
C_2(t) &= \frac{\sqrt{2}\xi^2}{(\Delta_L + \Delta_F - i\frac{\gamma}{2})} \left\{ \frac{1 - \exp[-i(2\Delta_L + 2\Delta_F + 2U - i\gamma)t]}{(2\Delta_L + 2\Delta_F + 2U - i\gamma)} - \frac{\exp[-i(\Delta_L + \Delta_F - i\frac{\gamma}{2})t]}{(\Delta_L + \Delta_F + 2U - i\frac{\gamma}{2})} \right\} \\
& + \sqrt{2}\xi^2 \frac{\exp[-i(2\Delta_L + 2\Delta_F + 2U - i\gamma)t]}{(\Delta_L + \Delta_F - i\frac{\gamma}{2})(\Delta_L + \Delta_F + 2U - i\frac{\gamma}{2})},
\end{aligned}$$

$$\begin{aligned}
C_3(t) = & -\sqrt{6}\xi^3 \frac{\{1 - \exp[-i(3\Delta_L + 3\Delta_F + 6U - i\frac{3\gamma}{2})t]\}}{(\Delta_L + \Delta_F - i\frac{\gamma}{2})(2\Delta_L + 2\Delta_F + 2U - i\gamma)(3\Delta_L + 3\Delta_F + 6U - i\frac{3\gamma}{2})} \\
& + \sqrt{6}\xi^3 \frac{\{\exp[-i(2\Delta_L + 2\Delta_F + 2U - i\gamma)t] - \exp[-i(3\Delta_L + 3\Delta_F + 6U - i\frac{3\gamma}{2})t]\}}{(\Delta_L + \Delta_F - i\frac{\gamma}{2})(2\Delta_L + 2\Delta_F + 2U - i\gamma)(\Delta_L + \Delta_F + 4U - i\frac{\gamma}{2})} \\
& + \sqrt{6}\xi^3 \frac{\{\exp[-i(\Delta_L + \Delta_F - i\frac{\gamma}{2})t] - \exp[-i(3\Delta_L + 3\Delta_F + 6U - i\frac{3\gamma}{2})t]\}}{(\Delta_L + \Delta_F - i\frac{\gamma}{2})(\Delta_L + \Delta_F + 2U - i\frac{\gamma}{2})(2\Delta_L + 2\Delta_F + 6U - i\gamma)} \\
& - \sqrt{6}\xi^3 \frac{\{\exp[-i(2\Delta_L + 2\Delta_F + 2U - i\gamma)t] - \exp[-i(3\Delta_L + 3\Delta_F + 6U - i\frac{3\gamma}{2})t]\}}{(\Delta_L + \Delta_F - i\frac{\gamma}{2})(\Delta_L + \Delta_F + 2U - i\frac{\gamma}{2})(\Delta_L + \Delta_F + 4U - i\frac{\gamma}{2})},
\end{aligned}$$

and for the infinite-time limit $\exp(-At) \rightarrow 0$ ($t \rightarrow \infty$), we have:

$$\begin{aligned}
C_0(\infty) & \equiv C_0 = 1, \\
C_1(\infty) & \equiv C_1 = \frac{-\xi}{(\Delta_L + \Delta_F - i\frac{\gamma}{2})}, \\
C_2(\infty) & \equiv C_2 = \frac{-\sqrt{2}\xi C_1}{(2\Delta_L + 2\Delta_F + 2U - i\gamma)}, \\
C_3(\infty) & \equiv C_3 = \frac{-\sqrt{3}\xi C_2}{(3\Delta_L + 3\Delta_F + 6U - i\frac{3\gamma}{2})}.
\end{aligned} \tag{S88}$$

For the state given in Eq. (S65), the infinite-time state (steady state) of the system reads as

$$\begin{aligned}
|\varphi(t \rightarrow \infty)\rangle = & |0\rangle + \frac{-\xi}{(\Delta_L + \Delta_F - i\frac{\gamma}{2})}|1\rangle + \frac{\sqrt{2}\xi^2}{(\Delta_L + \Delta_F - i\frac{\gamma}{2})(2\Delta_L + 2\Delta_F + 2U - i\gamma)}|2\rangle \\
& + \frac{-\sqrt{6}\xi^3}{(\Delta_L + \Delta_F - i\frac{\gamma}{2})(2\Delta_L + 2\Delta_F + 2U - i\gamma)(3\Delta_L + 3\Delta_F + 6U - i\frac{3\gamma}{2})}|3\rangle,
\end{aligned} \tag{S89}$$

and the normalization constant of the state is given by

$$N = 1 + |C_1|^2 + |C_2|^2 + |C_3|^2, \tag{S90}$$

where:

$$|C_1|^2 = \left| \frac{\xi}{(\Delta_L + \Delta_F - i\frac{\gamma}{2})} \right|^2 = \frac{\xi^2}{(\Delta_L + \Delta_F - i\frac{\gamma}{2})(\Delta_L + \Delta_F + i\frac{\gamma}{2})} = \frac{\xi^2}{[(\Delta_L + \Delta_F)^2 + \frac{\gamma^2}{4}]}, \tag{S91}$$

$$\begin{aligned}
|C_2|^2 & = \left| \frac{\sqrt{2}\xi^2}{(\Delta_L + \Delta_F - i\frac{\gamma}{2})(2\Delta_L + 2\Delta_F + 2U - i\gamma)} \right|^2 \\
& = \frac{2\xi^4}{(\Delta_L + \Delta_F - i\frac{\gamma}{2})(\Delta_L + \Delta_F + i\frac{\gamma}{2})(2\Delta_L + 2\Delta_F + 2U - i\gamma)(2\Delta_L + 2\Delta_F + 2U + i\gamma)} \\
& = \frac{2\xi^4}{[(\Delta_L + \Delta_F)^2 + \frac{\gamma^2}{4}][4(\Delta_L + \Delta_F + U)^2 + \gamma^2]},
\end{aligned} \tag{S92}$$

$$\begin{aligned}
|C_3|^2 & = \left| \frac{-\sqrt{6}\xi^3}{(\Delta_L + \Delta_F - i\frac{\gamma}{2})(2\Delta_L + 2\Delta_F + 2U - i\gamma)(3\Delta_L + 3\Delta_F + 6U - i\frac{3\gamma}{2})} \right|^2 \\
& = \frac{6\xi^6}{|\Delta_L + \Delta_F - i\frac{\gamma}{2}|^2 |(2\Delta_L + 2\Delta_F + 2U - i\gamma)|^2 |3\Delta_L + 3\Delta_F + 6U - i\frac{3\gamma}{2}|^2} \\
& = \frac{6\xi^6}{[(\Delta_L + \Delta_F)^2 + \frac{\gamma^2}{4}][4(\Delta_L + \Delta_F + U)^2 + \gamma^2][9(\Delta_L + \Delta_F + 2U)^2 + \frac{9\gamma^2}{4}]}.
\end{aligned} \tag{S93}$$

The probabilities of finding single, two and three photons in the cavity are, respectively, given by:

$$P_1 = \frac{|C_1|^2}{N}, \quad (\text{S94})$$

$$P_2 = \frac{|C_2|^2}{N}, \quad (\text{S95})$$

$$P_3 = \frac{|C_3|^2}{N}. \quad (\text{S96})$$

As mentioned in Sec. S2B, the equal-time third-order correlation function can be written as

$$g^{(3)}(0,0) \equiv g^{(3)}(0) \equiv \frac{\langle a^\dagger a^3 \rangle}{\langle \hat{a}^\dagger \hat{a} \rangle^3} = \frac{\langle \hat{a}^\dagger \hat{a} (\hat{a}^\dagger \hat{a} - 1) (\hat{a}^\dagger \hat{a} - 2) \rangle}{\langle \hat{a}^\dagger \hat{a} \rangle^3} = \frac{\langle (\hat{a}^\dagger \hat{a})^3 - 3(\hat{a}^\dagger \hat{a})^2 + 2\hat{a}^\dagger \hat{a} \rangle}{\langle \hat{a}^\dagger \hat{a} \rangle^3}$$

When the cavity field is in the state (S65), we have

$$\begin{aligned} g^{(3)}(0) &= \frac{\sum_{n,n'=0}^3 C_{n'}^* C_n \langle n' | (\hat{a}^\dagger \hat{a})^3 | n \rangle - 3 \sum_{n,n'=0}^3 C_{n'}^* C_n \langle n' | (\hat{a}^\dagger \hat{a})^2 | n \rangle + 2 \sum_{n,n'=0}^3 C_{n'}^* C_n \langle n' | \hat{a}^\dagger \hat{a} | n \rangle}{\left(\sum_{n,n'=0}^3 C_{n'}^* C_n \langle n' | \hat{a}^\dagger \hat{a} | n \rangle \right)^3} \\ &= \frac{|C_1|^2 + 8|C_2|^2 + 27|C_3|^2 - 3(|C_1|^2 + 4|C_2|^2 + 9|C_3|^2) + 2(|C_1|^2 + 2|C_2|^2 + 3|C_3|^2)}{(|C_1|^2 + 2|C_2|^2 + 3|C_3|^2)^3} \\ &= \frac{N(P_1 + 8P_2 + 27P_3 - 3P_1 - 12P_2 - 27P_3 + 2P_1 + 4P_2 + 6P_3)}{N^2(P_1 + 2P_2 + 3P_3)^3} \\ &= \frac{6P_3}{N(P_1 + 2P_2 + 3P_3)^3} \end{aligned}$$

In the weak-driving regime, we have the following approximate amplitudes: $C_0 \sim 1$, $C_1 \sim \xi/\gamma$, $C_2 \sim \xi^2/\gamma^2$, and $C_3 \sim \xi^3/\gamma^3$, i.e., $N \sim 1$ with $|C_3|^2 \ll |C_2|^2 \ll |C_1|^2 \ll 1$. Hence, the third-order correlation function can be written as

$$g^{(3)}(0) \approx \frac{6P_3}{P_1^3}. \quad (\text{S97})$$

Substituting Eqs. (S94) and (S96) into Eq. (S97), we can easily obtain

$$\begin{aligned} g^{(3)}(0) &\approx \frac{36\xi^6}{\left[(\Delta_L + \Delta_F)^2 + \frac{\gamma^2}{4} \right] \left[4(\Delta_L + \Delta_F + U)^2 + \gamma^2 \right] \left[9(\Delta_L + \Delta_F + 2U)^2 + \frac{9\gamma^2}{4} \right]} \cdot \frac{\left[(\Delta_L + \Delta_F)^2 + \frac{\gamma^2}{4} \right]^3}{\xi^6} \\ &= \frac{\left[(\Delta_L + \Delta_F)^2 + \frac{\gamma^2}{4} \right]^2}{\left[(\Delta_L + \Delta_F + U)^2 + \frac{\gamma^2}{4} \right] \left[(\Delta_L + \Delta_F + 2U)^2 + \frac{\gamma^2}{4} \right]}, \quad (\text{S98}) \end{aligned}$$

where $\Delta_F > 0$ ($\Delta_F < 0$) denotes the light propagating against (along) the direction of the spinning resonator.

Here, we focus on the non-spinning case ($\Delta_F = 0$), the rotating case is discussed in Sec. S4. For this case, the third-order correlation function becomes

$$g_0^{(3)}(0) = \frac{(\Delta_L^2 + \gamma^2/4)^2}{\left[(\Delta_L + U)^2 + \gamma^2/4 \right] \left[(\Delta_L + 2U)^2 + \gamma^2/4 \right]}. \quad (\text{S99})$$

Including the second-order correlation function, we can quantitatively compare our analytical results with numerical calculations [S21, S22]. We find an excellent agreement between the numerical calculations and the approximate analytical solutions, as shown in Fig. S6. Here, the solid curves are plotted using the numerical solution, while the curves with symbols are based on the analytical solution given in Eqs. (S62) and (S99). As for the $g_0^{(2)}(0) \approx 2P(2)/P(1)^2$, given in Eq. (S60), the dip $D^{(2)}$ and the peak $P^{(2)}$ in the light green curves correspond to the single- and two-photon resonant driving cases, respectively. In the single-photon resonant driving case ($k = 1$), a single

photon can be resonantly injected into the cavity, while the probability of finding two photons in the cavity is largely suppressed due to the energy restriction; this represents 1PB. We find that the analytical value of $g_0^{(2)}(0) \sim 0.0008$ at this dip $D^{(2)}$, which is well-matched with our numerical value $g_0^{(2)}(0) \sim 0.0009$. In the two-photon resonant driving case ($k = 2$), the probability for finding two photons inside the cavity is resonantly enhanced, and this corresponds to a peak in the curve of $g^{(2)}(0)$. We find that the analytical value of $g^{(2)}(0) \sim 974$ at this peak $P^{(2)}$ is above the numerical solution $g^{(2)}(0) \sim 673$, since we neglected the two-photon probability in the denominator of the analytical formula [this can be seen more clearly in Eqs. (S59) and (S62)]. As for the $g_0^{(3)}(0) \approx 6P(3)/P(1)^3$, given in Eq. (S97), the dip $D^{(3)}$ and the peaks $P_1^{(3)}$ and $P_2^{(3)}$ in the dark green curves correspond to the single-, two-, and three-photon resonant-driving cases, respectively. In the single-photon resonant-driving case ($k = 1$), $P(1) \gg P(2) \gg P(3)$, thus, there is a dip [i.e., $D^{(3)}$] in the $g_0^{(3)}(0)$ curve. For the two-photon resonant-driving case ($k = 2$), the single-photon probability is suppressed, which causes the occurrence of the peak $P_1^{(3)}$. However, the peak $P_1^{(3)}$ is lower than the peak $P_2^{(3)}$ at $k = 3$, since the three-photon probability is enhanced at $k = 3$ (i.e., three-photon resonant-driving case), but still suppressed at $k = 2$ (i.e., two-photon resonant-driving case).

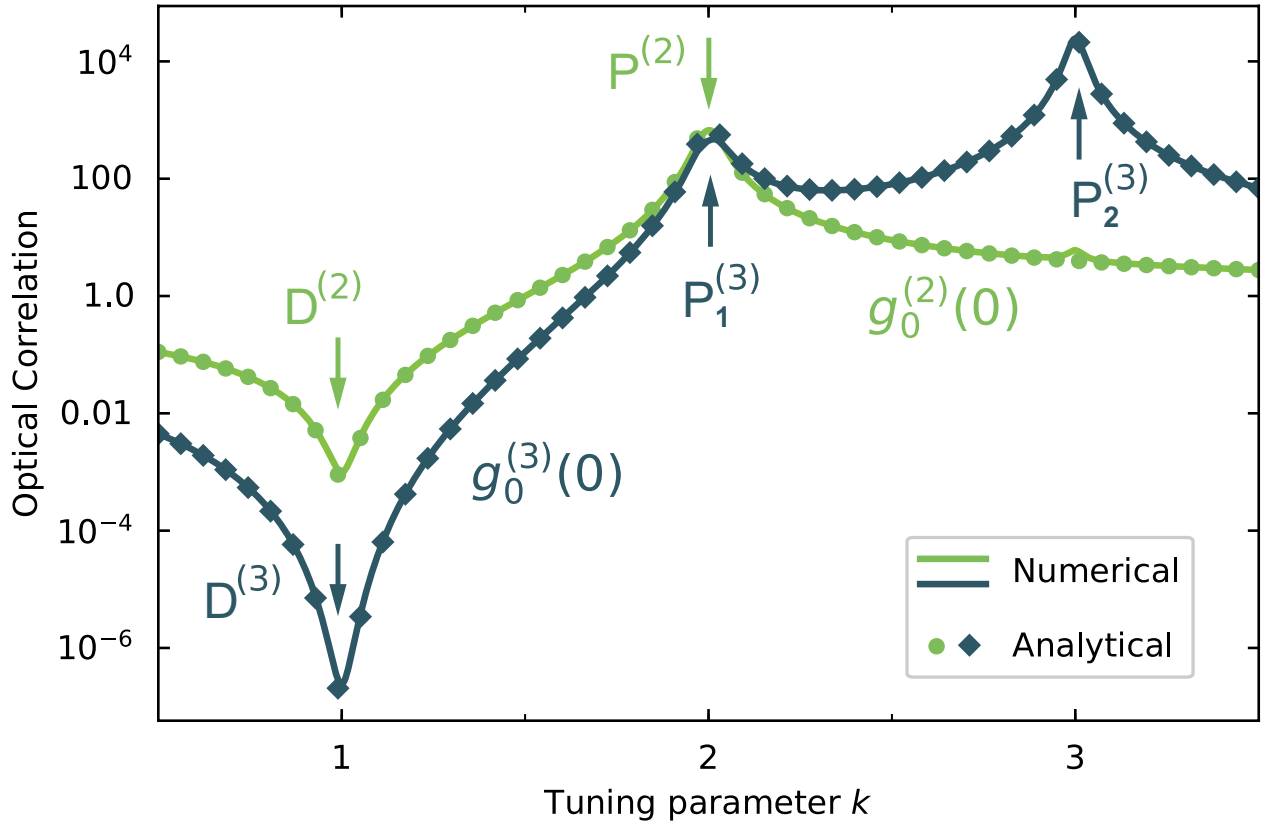


FIG. S6. The second- and third-order correlation functions versus the tuning parameter k for the non-spinning resonator case. The symbols denote our approximate analytical results [$g_0^{(2)}(0)$ given in Eq. (S62), $g_0^{(3)}(0)$ given in Eq. (S99)], while the solid curves correspond to our numerical results. Here, $D^{(2)}$ [$D^{(3)}$] is the dip in the $g_0^{(2)}(0)$ [$g_0^{(3)}(0)$] curves; $P^{(2)}$ and $P^{(3)}$ are the peaks in the $g_0^{(2)}(0)$ and $g_0^{(3)}(0)$ curves, respectively. The parameters used here are the same as those in Fig. S4.

S4. ROTATION-INDUCED QUANTUM NONRECIPROcity

A. Rotation-induced shifts

For the optical microtoroid resonator, an input-laser light applied from the left or right side of the cavity causes a clockwise (CW) circulating mode or a counterclockwise (CCW) circulating mode. When the microresonator is rotating, $\Delta_F > 0$ and $\Delta_F < 0$ denote the cases with the light propagating against and along the spinning direction of the resonator, respectively, i.e., for the CCW spinning resonator, $\Delta_F > 0$ ($\Delta_F < 0$) indicates an input-laser applied from the left (right) side; for the CW spinning resonator, $\Delta_F > 0$ ($\Delta_F < 0$) indicates an input-laser used from the right (left) side.

When the resonator is rotating, the second-order correlation function in Eq. (S61) can be written as

$$g_{\pm}^{(2)}(0) = \frac{(\Delta_L \pm |\Delta_F|)^2 + \gamma^2/4}{(\Delta_L \pm |\Delta_F| + U)^2 + \gamma^2/4}, \quad (\text{S100})$$

where $g_{-}^{(2)}(0)$ [$g_{+}^{(2)}(0)$] denotes the equal-time second-order correlation function for $\Delta_F < 0$ ($\Delta_F > 0$).

For the $\Delta_F < 0$ case, 1PB emerges at $\Delta_L = |\Delta_F|$ with $g_{-}^{(2)}(0) = (\gamma^2/4)/(U^2 + \gamma^2/4) = [4(U/\gamma)^2 + 1]^{-1}$. This minimum value of $g_{-}^{(2)}(0)$ is independent of the angular speed Ω ; thus, the minimum value of $g_{-}^{(2)}(0)$ is a constant. Since $|\Delta_F|$ is an amount proportional to the angular speed Ω , the dip $D^{(2)}$ experiences linearly shifts with Ω . Also, $D^{(2)}$ experiences linearly shifts to the opposite direction for the $\Delta_F < 0$ case, since now 1PB emerges at $\Delta_L = -|\Delta_F|$. The shifts of the curve can also be understood from an energy-level structure, where the rotation of the resonator causes upper or lower shifts of energy levels, as shown in Fig. S3.

Here, we plot the correlation function $g^{(2)}(0)$ as a function of k when the angular speed Ω takes various values, as shown in Fig. S7. For the $\Delta_F < 0$ case, a blue shift of the $g^{(2)}(0)$ curve can be clearly seen in Fig. S7(a). For the $\Delta_F > 0$ case, a red shift can be seen in Fig. S7(b). This indicates a highly-tunable nonreciprocal PB device, i.e., *sub-Poissonian* light can be achieved by driving from one side; *super-Poissonian* light emerges by driving from the opposite side (see Fig. 2 in the main article).

For example, let us now fix the CCW rotation of the resonator; hence $\Delta_F > 0$ ($\Delta_F < 0$) corresponds to the situation of driving the resonator from its left (right) side, i.e., the CW (CCW) mode frequency is $\omega_{\odot} \equiv \omega_0 + |\Delta_F|$ ($\omega_{\ominus} \equiv \omega_0 - |\Delta_F|$), as aforementioned. When the optical resonator rotates with an angular velocity $\Omega = 6.6$ kHz [S6], we find $g_{\odot}^{(2)}(0) \sim 0.39$ and $g_{\ominus}^{(2)}(0) \sim 2.53$, i.e., *sub-Poissonian* light can be achieved by driving the device from its left side, while *super-Poissonian* light emerges by driving from the right side, as shown in Fig. S8.

The third-order correlation function Eq. (S98) in the rotating resonator becomes

$$g_{\pm}^{(3)}(0) = \frac{[(\Delta_L \pm |\Delta_F|)^2 + \gamma^2/4]^2}{[(\Delta_L \pm |\Delta_F| + U)^2 + \gamma^2/4][(\Delta_L \pm |\Delta_F| + 2U)^2 + \gamma^2/4]}, \quad (\text{S101})$$

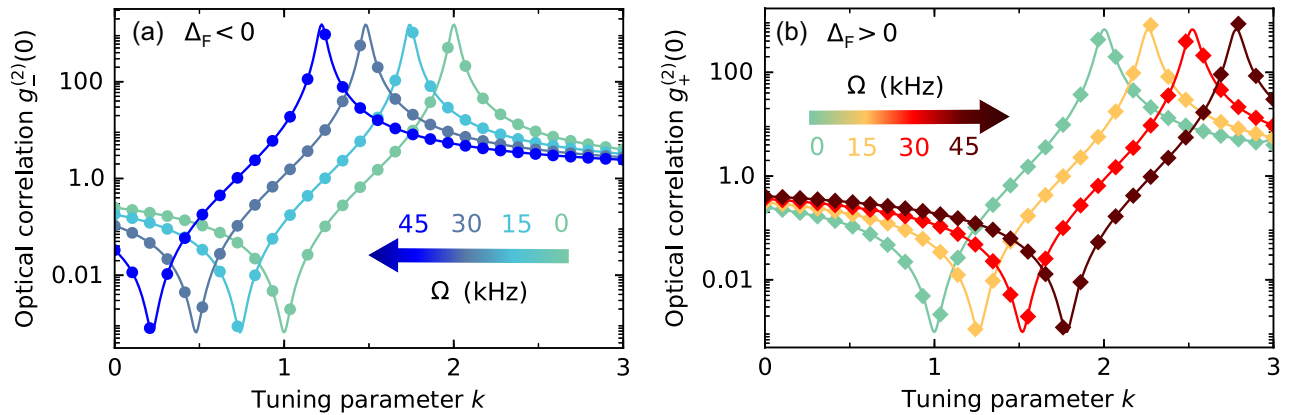


FIG. S7. Dependence of the equal-time second-order correlation functions $g_{\pm}^{(2)}(0)$ on the tuning parameter k for various values of the angular speed Ω . The symbols are our approximate analytical results given in Eq. (S100), while the solid curves are our numerical results. The other parameters used here are the same as those in Fig. S4.

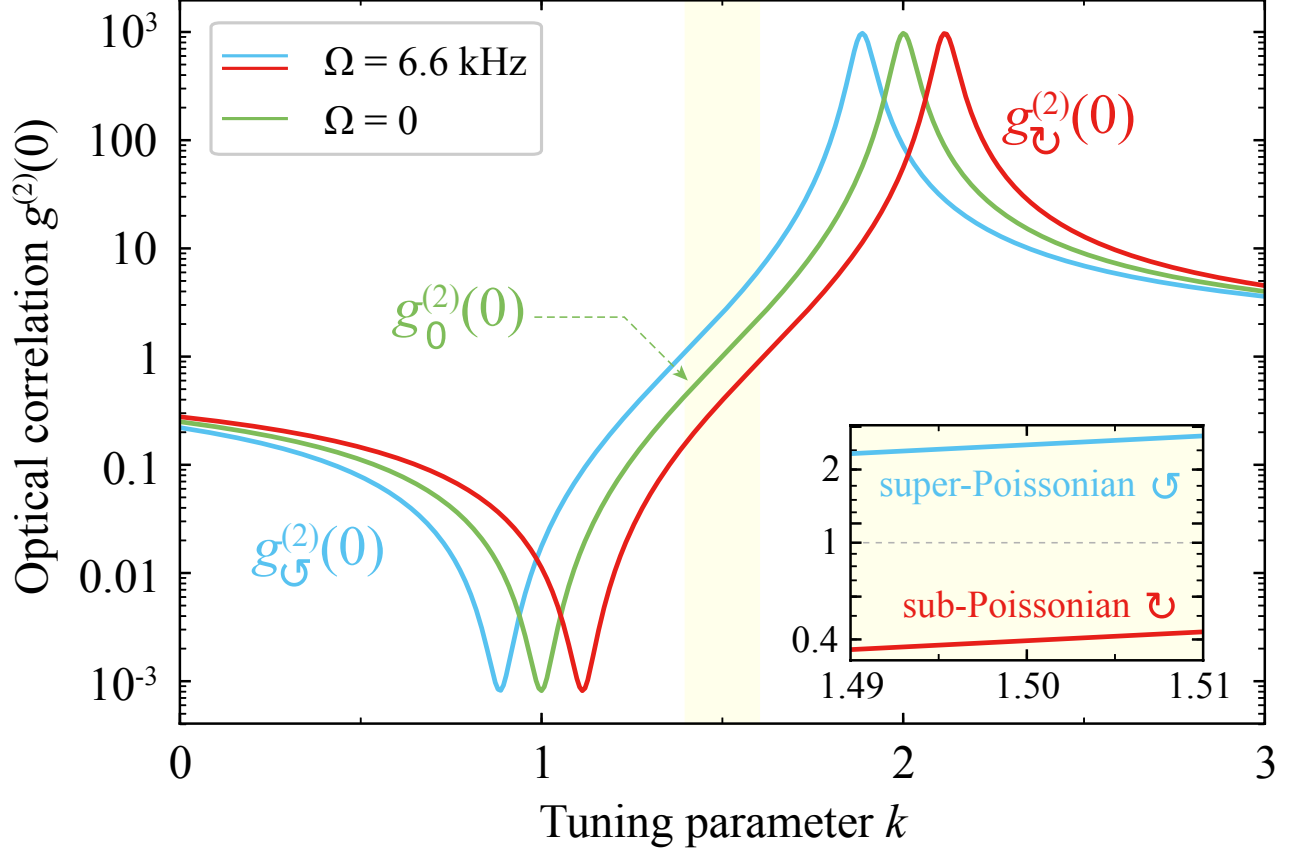


FIG. S8. Second-order correlation function $g^{(2)}(0)$ versus the tuning parameter k for different input directions. At $k = 1.5$, sub- and super-Poissonian light can be achieved by driving the device from its left (red curve) and right (blue curve) sides, respectively. Here, we assume that the angular velocity is $\Omega = 6.6$ kHz [S6] ($\Omega = 0$) for the spinning (non-spinning) resonator. The other parameter values are the same as those in the main text.

where $g_{-}^{(3)}(0)$ ($g_{+}^{(3)}(0)$) denotes the third-order optical intensity correlation for the $\Delta_F < 0$ ($\Delta_F > 0$) case. Similarly, the curve of $g^{(3)}(0)$ also experiences opposite shifts for different driving directions.

B. Nonreciprocal photon blockade

We have investigated PB effects (witnessing sub-Poissonian light) and photon-induced tunneling (PIT, corresponding to super-Poissonian light) for the non-spinning case in the former Sections. Note that PB and PIT always emerge at fixed locations of the tuning parameter k , no matter if the input-laser comes from the left or right side (see Figs. S4 and S5). However, the rotation of the resonator can lead to upper or lower shifts of energy levels for different driving directions, as discussed in Sec. S4A. Therefore, using a spinning nonlinear optical resonator, under the same driving frequencies, PIT can emerge by driving from one side and 1PB/2PB can emerge by driving from the other direction, i.e., *unidirectional* 1PB/2PB. Furthermore, 1PB for driving from one side and 2PB for driving from the opposite direction can also be realized with this spinning device.

As shown in Figs. S9(a) and S9(b), when the angular speed of the resonator is $\Omega = 58$ kHz, we find (i) 1PB for $\Delta_F > 0$ and PIT for $\Delta_F < 0$, at $k = 2.0$; (ii) 2PB for $\Delta_F > 0$ and PIT for $\Delta_F < 0$, at $k = 3.0$. These nonreciprocal 1PB and 2PB can also be confirmed by comparing the photon-number distribution $P(n)$ with the Poissonian distribution $\mathcal{P}(n)$. Figure S9(b) shows that: (i) single-photon probability $P(1)$ is enhanced while two- and more-photon probabilities $P(m > 1)$ are suppressed for the $\Delta_F > 0$ case, leading to 1PB; in contrast, $P(1)$ is suppressed while $P(m > 1)$ are enhanced for the $\Delta_F < 0$ case, leading to PIT. (ii) only two-photon probability $P(2)$ is enhanced for $\Delta_F > 0$, which corresponds to 2PB; in contrast, PIT emerges for $\Delta_F < 0$. The unidirectional 2PB can also be achieved at

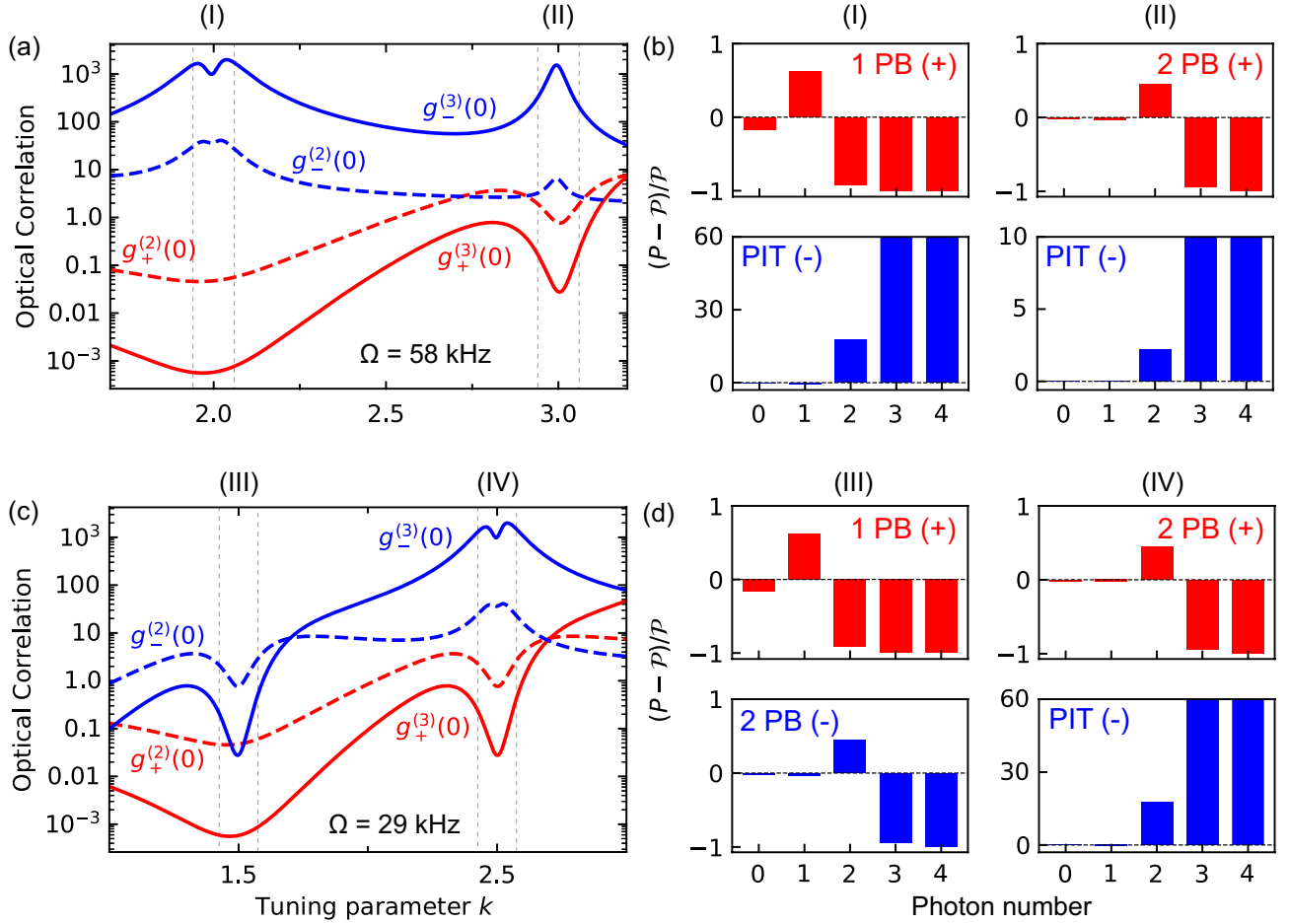


FIG. S9. Optical intensity correlation functions $g_{\pm}^{(2)}(0)$ (dashed curves) and $g_{\pm}^{(3)}(0)$ (solid curves) versus the tuning parameter k for different driving directions. Different cases of nonreciprocal PB can be achieved for different angular speeds (a,b) $\Omega = 58$ kHz and (c,d) $\Omega = 29$ kHz. These effects can also be recognized from (b,d) the deviations of the photon distribution to the standard Poissonian distribution with the same mean photon number [i.e., Eq. (S13)]. The panels (b) and (d) correspond to panels (a) and (c), respectively. Here, ‘PIT’ is photon-induced tunneling, and the other parameters used here are the same as those in Fig. S5.

$k = 2.5$ when $\Omega = 29$ kHz, as shown in Figs. S9(c) and S9(d). Such *quantum* nonreciprocities indicate one-way quantum devices at the few-photon level, and open up exciting prospects for applications in nonreciprocal quantum technologies, such as nonreciprocal quantum information processing or few-photon topological devices [S23–S25].

More interestingly, when the angular speed of the nonlinear optical resonator is $\Omega = 29$ kHz, 2PB emerges at $k = 1.5$ for $\Delta_F < 0$, while 1PB emerges with the same driving strength for $\Delta_F > 0$, as shown in Figs. S9(c) and S9(d). In contrast to the nonreciprocities of the former cases between the sub- and super-Poissonian states of light, this is a new kind of nonreciprocal PB between two sub-Poissonian states of light, indicating possible applications for few-photon nonreciprocal devices with direction-dependent counting-statics.

All of the cases of nonreciprocal PB can be intuitively understood by considering the energy-level structure of the system. As shown in Fig. S3(a), for the $\Delta_F > 0$ case, when angular speed fulfills $|\Delta_F| = U$ and the probe light with frequency $\omega_0 + |\Delta_F|$ ($k = 2.0$), the light is resonantly coupled to the transition $|0\rangle \rightarrow |1\rangle$. The transition $|1\rangle \rightarrow |2\rangle$ is detuned by $2\hbar U$ and, thus, suppressed for $U > \gamma$, i.e., once, a photon is coupled into the resonator, it suppresses the probability of the second photon with the same frequency going into the resonator. In contrast, for the $\Delta_F < 0$ case, there is a three-photon resonance with the transition $|0\rangle \rightarrow |3\rangle$, hence the absorption of the first photon favors also that of the second or subsequent photons, i.e., resulting in PIT. This is a clear signature of nonreciprocal 1PB, i.e., *sub-Poissonian* light emerges for $\Delta_F > 0$, while *super-Poissonian* light can be observed for $\Delta_F < 0$.

As shown in Figs. S3(c) [S3(e)], for the $\Delta_F > 0$ case, by choosing $|\Delta_F| = U$ ($|\Delta_F| = U/2$) and $\Delta_L = -2U$ ($\Delta_L = -3U/2$), the transition $|0\rangle \rightarrow |2\rangle$ is resonantly driven by the input laser, but the transition $|2\rangle \rightarrow |3\rangle$ is

TABLE II. Different cases of nonreciprocal PB effects in a spinning resonator for $P_{\text{in}} = 0.3$ pw. Here, photon-induced tunneling (PIT) corresponds to an n -photon resonance (n PR).

No.	$\Delta_F > 0$	$\Delta_F < 0$	Conditions	Parameters
(1)	1PB	PIT (3PR)	$\Delta_F = \pm U, \Delta_L = -U$	$\Omega = 58$ kHz, $k = 2.0$
(2)	PIT (3PR)	1PB	prohibited	
(3)	2PB	PIT (4PR)	$\Delta_F = \pm U, \Delta_L = -2U$	$\Omega = 58$ kHz, $k = 3.0$
(4)	PIT (4PR)	2PB	prohibited	
(5)	2PB	PIT (3PR)	$\Delta_F = \pm U/2, \Delta_L = -3U/2$	$\Omega = 29$ kHz, $k = 2.5$
(6)	PIT (3PR)	2PB	prohibited	
(7)	1PB	2PB	$\Delta_F = \pm U/2, \Delta_L = -U/2$	$\Omega = 29$ kHz, $k = 1.5$
(8)	2PB	1PB	prohibited	

detuned by $4\hbar U$, which features the 2PB effect; in contrast, for the $\Delta_F < 0$ case, four-photon resonance (three-photon resonance) happens for the transition $|0\rangle \rightarrow |4\rangle$ ($|0\rangle \rightarrow |3\rangle$), leading to PIT. This is also a nonreciprocal PB.

As shown in Fig. S3(g), for the $\Delta_F > 0$ case, when $|\Delta_F| = U/2$ and $\Delta_L = -U/2$ ($k = 1.5$), the input light is resonantly coupled to the transition $|0\rangle \rightarrow |1\rangle$, and the transition $|1\rangle \rightarrow |2\rangle$ is detuned by $2\hbar U$, leading to 1PB. More interestingly, for the $\Delta_F < 0$ case, the input light is just resonantly coupled to the transition $|0\rangle \rightarrow |2\rangle$, and the transition $|2\rangle \rightarrow |3\rangle$ is detuned by $4\hbar U$, i.e., resulting in 2PB. This 1PB-2PB nonreciprocity can suggest an application for a purely quantum device with *direction-dependent counting statistics*. This new nonreciprocal feature, which (to our knowledge) has not been revealed previously.

Table II shows different cases of nonreciprocal PB. Interestingly, both PB-PIT and 1PB-2PB nonreciprocities can only occur in an irreversible way. Unidirectional 1PB for $\Delta_F > 0$, i.e., 1PB emerges for $\Delta_F > 0$ and PIT emerges for $\Delta_F < 0$, can occur with the same angular speeds ($\Delta_F = \pm U$), and the same driving frequencies ($\Delta_L = -U$). However, the case of PIT for $\Delta_F > 0$ and 1PB for $\Delta_F < 0$ cannot be observed with the same angular speeds and driving frequencies, i.e., one-way 1PB is an irreversible quantum nonreciprocal effect. Also, 1PB-2PB nonreciprocity can only happen in the case of 1PB for $\Delta_F > 0$ and 2PB for $\Delta_F < 0$, but *not vice versa*.

Note that 1PB and 2PB correspond to the single- and two-photon resonances, respectively. PIT is also caused by a multi-photon resonance. The multi-photon resonance can be clearly seen in energy-level diagrams, thus, the origin of this irreversible feature can be understood from the energy-level diagrams for $\Delta_F > 0$ and $\Delta_F < 0$. Without the rotation, the energy-level diagrams for the $\Delta_F > 0$ and $\Delta_F < 0$ cases are symmetric. Due to the rotation, energy levels experience shifts to different directions for $\Delta_F > 0$ and $\Delta_F < 0$, leading to asymmetries of energy-level diagrams, as shown in Fig. S3. From Sec. S2 A, the energy levels of this spinning system are $E_n = n\hbar\Delta_L + n\hbar\Delta_F + (n^2 - n)\hbar U$. Thus, we have

$$E_n/n = \hbar(\Delta_L + \Delta_F) + (n - 1)\hbar U. \quad (\text{S102})$$

Then the driving frequency of an n -photon resonance for the $\Delta_F > 0$ case is

$$\omega_L = \omega_0 + |\Delta_F| + nU - U, \quad (\text{S103})$$

and the driving frequency of an m -photon resonance for the $\Delta_F < 0$ case is

$$\omega'_L = \omega_0 - |\Delta_F| + mU - U. \quad (\text{S104})$$

Under the same driving frequency, we have

$$\begin{aligned} \omega_0 + |\Delta_F| + nU - U &= \omega_0 - |\Delta_F| + mU - U \\ |\Delta_F| + nU &= -|\Delta_F| + mU \\ 2|\Delta_F| &= (m - n)U. \end{aligned} \quad (\text{S105})$$

Because $|\Delta_F| > 0$ (i.e., $\Omega \neq 0$) and $U > 0$, we have the following condition for the allowed cases of nonreciprocal PB

$$n < m. \quad (\text{S106})$$

When the driving frequencies for $\Delta_F > 0$ and $\Delta_F < 0$ are the same, an n -photon resonance for $\Delta_F > 0$ and an m -photon resonance for $\Delta_F < 0$ can only happen under the condition $n < m$. In contrast to this, the cases of $n > m$ are prohibited, as shown in Figs. S3(b), S3(d), S3(f), and S3(h).

*Corresponding author.
jinghui73@foxmail.com

-
- [S1] G. J. Milburn, “Quantum and classical Liouville dynamics of the anharmonic oscillator,” *Phys. Rev. A* **33**, 674 (1986).
- [S2] W. Leoński and R. Tanaś, “Possibility of producing the one-photon state in a kicked cavity with a nonlinear Kerr medium,” *Phys. Rev. A* **49**, R20 (1994).
- [S3] A. Imamoglu, H. Schmidt, G. Woods, and M. Deutsch, “Strongly interacting photons in a nonlinear cavity,” *Phys. Rev. Lett.* **79**, 1467 (1997).
- [S4] A. Miranowicz, M. Paprzycka, Y.-x. Liu, J. Bajer, and F. Nori, “Two-photon and three-photon blockades in driven nonlinear systems,” *Phys. Rev. A* **87**, 023809 (2013).
- [S5] G. B. Malykin, “The Sagnac effect: correct and incorrect explanations,” *Phys. Usp.* **43**, 1229 (2000).
- [S6] S. Maayani, R. Dahan, Y. Kligerman, E. Moses, A. U. Hassan, H. Jing, F. Nori, D. N. Christodoulides, and T. Carmon, “Flying couplers above spinning resonators generate irreversible refraction,” *Nature (London)* **558**, 569 (2018).
- [S7] A. Majumdar, M. Bajcsy, and J. Vučković, “Probing the ladder of dressed states and nonclassical light generation in quantum-dot-cavity QED,” *Phys. Rev. A* **85**, 041801 (2012).
- [S8] S. S. Shamlou, A. S. Parkins, M. J. Collett, and H. J. Carmichael, “Multi-photon blockade and dressing of the dressed states,” *Opt. Commun.* **283**, 766 (2010).
- [S9] A. Miranowicz, J. Bajer, M. Paprzycka, Y.-x. Liu, A. M. Zagoskin, and F. Nori, “State-dependent photon blockade via quantum-reservoir engineering,” *Phys. Rev. A* **90**, 033831 (2014).
- [S10] H. J. Carmichael, “Breakdown of photon blockade: a dissipative quantum phase transition in zero dimensions,” *Phys. Rev. X* **5**, 031028 (2015).
- [S11] C. J. Zhu, Y. P. Yang, and G. S. Agarwal, “Collective multiphoton blockade in cavity quantum electrodynamics,” *Phys. Rev. A* **95** (2017).
- [S12] C. Hamsen, K. N. Tolazzi, T. Wilk, and G. Rempe, “Two-photon blockade in an atom-driven cavity QED system,” *Phys. Rev. Lett.* **118**, 133604 (2017).
- [S13] A. Faraon, I. Fushman, D. Englund, N. Stoltz, P. Petroff, and J. Vučković, “Coherent generation of non-classical light on a chip via photon-induced tunnelling and blockade,” *Nat. Phys.* **4**, 859 (2008).
- [S14] A. Majumdar, M. Bajcsy, A. Rundquist, and J. Vučković, “Loss-enabled sub-Poissonian light generation in a bimodal nanocavity,” *Phys. Rev. Lett.* **108** (2012).
- [S15] X.-W. Xu, Y.-J. Li, and Y.-x. Liu, “Photon-induced tunneling in optomechanical systems,” *Phys. Rev. A* **87**, 025803 (2013).
- [S16] A. Rundquist, M. Bajcsy, A. Majumdar, T. Sarmiento, K. Fischer, K. G. Lagoudakis, S. Buckley, A. Y. Piggott, and J. Vučković, “Nonclassical higher-order photon correlations with a quantum dot strongly coupled to a photonic-crystal nanocavity,” *Phys. Rev. A* **90** (2014).
- [S17] K. M. Birnbaum, A. Boca, R. Miller, A. D. Boozer, T. E. Northup, and H. J. Kimble, “Photon blockade in an optical cavity with one trapped atom,” *Nature (London)* **436**, 87 (2005).
- [S18] R. J. Glauber, *Quantum Theory of Optical Coherence* (Wiley-VCH, Weinheim, 2007).
- [S19] M. Wang, X.-Y. Lü, A. Miranowicz, T.-S. Yin, Y. Wu, and F. Nori, “Unconventional phonon blockade via atom-phonon-phonon interaction in hybrid optomechanical systems,” preprint arXiv:1806.03754 (2018).
- [S20] M. B. Plenio and P. L. Knight, “The quantum-jump approach to dissipative dynamics in quantum optics,” *Rev. Mod. Phys.* **70**, 101 (1998).
- [S21] J. R. Johansson, P. D. Nation, and F. Nori, “Qutip: An open-source Python framework for the dynamics of open quantum systems,” *Comput. Phys. Commun.* **183**, 1760 (2012).
- [S22] J. R. Johansson, P. D. Nation, and F. Nori, “Qutip 2: A Python framework for the dynamics of open quantum systems,” *Comput. Phys. Commun.* **184**, 1234 (2013).
- [S23] C. H. Bennett and D. P. DiVincenzo, “Quantum information and computation,” *Nature (London)* **404**, 247 (2000).
- [S24] I. Buluta, S. Ashhab, and F. Nori, “Natural and artificial atoms for quantum computation,” *Rep. Prog. Phys.* **74**, 104401 (2011).
- [S25] P. Lodahl, S. Mahmoodian, S. Stobbe, A. Rauschenbeutel, P. Schneeweiss, J. Volz, H. Pichler, and P. Zoller, “Chiral quantum optics,” *Nature (London)* **541**, 473 (2017).